Journal of Medicinal Chemistry

pubs.acs.org/jmc Article

Synthesis and Antichlamydial Activity of Molecules Based on Dysregulators of Cylindrical Proteases

Mohamed A. Seleem, Nathalia Rodrigues de Almeida, Yashpal Singh Chhonker, Daryl J. Murry, Zaira da Rosa Guterres, Amanda M. Blocker, Shiomi Kuwabara, Derek J. Fisher, Emilse S. Leal, Manuela R. Martinefski, Mariela Bollini, María Eugenia Monge, Scot P. Ouellette,* and Martin Conda-Sheridan*

Cite This: *J. Med. Chem.* 2020, 63, 4370−4387 Read Online

ACCESS | Metrics & More | Article Recommendations | Supporting Information

ABSTRACT: *Chlamydia trachomatis* is the most common sexually transmitted bacterial disease globally and the leading cause of infertility and preventable infectious blindness (trachoma) in the world. Unfortunately, there is no FDA-approved treatment specific for chlamydial infections. We recently reported two sulfonylpyridines that halt the growth of the pathogen. Herein, we present a SAR of the sulfonylpyridine molecule by introducing substituents on the aromatic regions. Biological evaluation studies showed that several analogues can impair the growth of *C. trachomatis* without affecting host cell viability. The compounds did not kill other bacteria, indicating selectivity for *Chlamydia*. The compounds presented mild toxicity toward mammalian cell lines. The compounds were found to be nonmutagenic in a *Drosophila melanogaster* assay and exhibited a promising stability in both plasma and gastric fluid. The presented results indicate this scaffold is a promising starting point for the development of selective antichlamydial drugs.

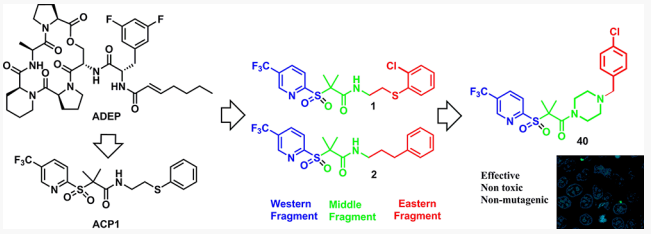

INTRODUCTION

Chlamydia trachomatis is a Gram-negative bacterium that infects 1.7 million people in the U.S. with an ∼8.8% increase in infection rates since 2013.[1,2] It is the most commonly reported bacterial sexually transmitted infection (STI) worldwide according to recent surveillance by the Centers for Disease Control and Prevention.[2,3] *Chlamydia*, which primarily targets epithelial cells, is considered the leading cause of infertility and preventable infectious blindness (trachoma) in the world.[4,5] Perhaps the most serious issue with chlamydial infections, and a chief cause of its deleterious consequences, is the asymptomatic nature of the infection.[6,7] Untreated chlamydial infections can result in chronic sequelae, such as pelvic inflammatory disease, which can lead to ectopic pregnancy and tubal factor infertility.[4]

The chlamydial developmental cycle commences by attachment of an infective, nonreplicative elementary body (EB) to the plasma membrane of the host cell. Within the host cell, the EB remains within a host-derived vesicle, termed an inclusion. Later the EB differentiates into its replicative form, the reticulate body (RB), which begins the replication process.[8,9] After multiple rounds of polarized division[10] within the inclusion, RBs undergo a secondary differentiation to EBs, and the pathogen is released from the host cell starting another round of infection[9,11]

Currently, there is no vaccine nor a selective drug approved by the FDA to treat *Chlamydia trachomatis*.[12,13] The first-line antibiotics used for chlamydia infections (i.e., azithromycin (AZM) and doxycycline) are broad spectrum drugs that can affect regular functions of the commensal microbiota and encourage the development of bacterial resistance.[14] In addition, *C. trachomatis* recurrence after antibiotic treatment remains a considerable issue that may eventually lead to treatment failure and the chronic sequelae associated with this pathogen.[15−17] For example, repeated chlamydial infections at rates of ∼25% for women and ∼20% for men have been reported after AZM treatment.[18] Taking into consideration the steady increase in infection cases, the risk of contagion, and the rise of general bacterial resistance due to untargeted treatments, the development of a selective chlamydial drug is needed to meet the challenges posed by this STI.

Several approaches are being pursued to develop specific treatments against chlamydial infections. Noteworthy is the seminal work of Almqvist et al. that sought to inhibit chlamydial growth by blocking the glucose-6-phosphate pathway.[19,20] This group has developed a novel class of

Received: March 2, 2020
Published: March 31, 2020

https://dx.doi.org/10.1021/acs.jmedchem.0c00371
J. Med. Chem. 2020, 63, 4370−4387

thiazolino-2-pyridones that show remarkable inhibitory activity and low toxicity toward mammalian cells. Elofsson and co-workers also reported another intriguing approach focused on blocking the type II fatty acid synthesis pathway (FAS II).[21] The same group has prepared compounds with dual activity by combining key features from active compounds into hybrid systems.[22] These important works highlight the importance of designing compounds that affect nontraditional bacterial targets to eradicate this pathogen.

Another antimicrobial target that has gathered considerable attention recently are the cylindrical proteases.[23,24] It has been suggested that dysregulation of proteolytic enzymes is a novel approach to treat bacterial infections[25−28] because the indiscriminate degradation of proteins can damage the physiology, pathogenicity, and cellular processes of the organism.[29,30] Previously, Brötz-Oesterhelt et al. reported some cyclic acyldepsipeptides (ADEP) (Figure 1) activate

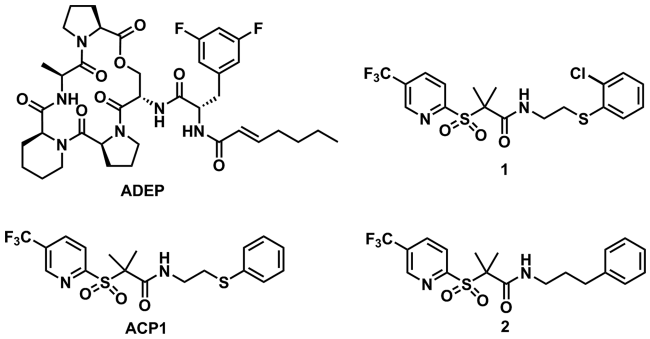

Figure 1. Structures of ADEP and ACP compounds.

ClpP, leading to the death of *Escherichia coli*.[25] Others expanded their findings showing that ClpP activation can kill other bacteria, including *Neisseria gonorrheae*, *Neisseria meningitidis*, *Haemophilus influenzae*, *Pseudomonas aeruginosa*, and *Staphylococcus aureus*, through various *in vitro* and *in vivo* assays.[31−35] Although promising, ADEPs possess some inherent limitations such as poor solubility, metabolic instability, fast clearance in animal studies, and challenging chemical synthesis.[36−38]

Building upon that precedent, Leung and co-workers combined computational chemistry and biochemical experiments to identify new scaffolds that can activate ClpP.[35] Two of the synthesized molecules, named ACP1a and b (**1** and **2**, Figure 1), showed moderate antibacterial activity against *N. meningitidis* (64 μg/mL and 16 μg/mL, respectively) and *H. influenzae* (32 μg/mL and 8 μg/mL respectively). Both molecules were 10−20-fold less potent than ADEP1. However, ACP1b was found to activate *E. coli* ClpP in an enzymatic assay, suggesting its potential as an antibiotic against this target.[35]

The biological functions of *Chlamydia* are also hypothesized to be regulated by cylindrical proteases, which degrade proteins and peptides to maintain homeostasis and perhaps to regulate differentiation of the developmental forms.[39−41] Recent work by us and others highlights the critical role of this degradation machinery in *Chlamydia*.[41,42] Four core Clp proteins have been identified in this organism: the caseinolytic proteases, ClpP1 and ClpP2, and two associated ATPase chaperones (AAA+) with diverse cellular activities,[43] ClpC and ClpX.[27,44,45] These chaperones bind to the axial faces of ClpP regulating its proteolytic activity. Using the work of Leung as a starting point, we synthesized molecules **1** and **2** and studied their ability to affect *C. trachomatis* as well as their effects on chlamydial growth and viability.[41] We found both compounds cause a drastic decrease in the formation of infectious EBs, although we could not definitively assign this effect to a disruption in ClpP activity in *Chlamydia*. Based on our early report, we decided to optimize compounds **1** and **2** to establish structure−activity relationships (SAR).

In the present work, we report the antichlamydial activity of new antichlamydial agents. One of the new molecules (compound **40**) was found to affect both chlamydial inclusion numbers, size, and morphology in infected HEp-2 cells. In addition, we performed the preliminary mechanism of action studies to understand the eradication process. We also investigated the antimicrobial activity of the compounds against several Gram-positive and Gram-negative bacteria, as well as fungi, to establish their spectrum of activity. Finally, we assessed the toxicity of various compounds toward human cells, their mutagenicity in *Drosophila melanogaster*, and their stability in mouse plasma, simulated gastric fluid, and human liver microsomes. The results indicate these new compounds are selective for *Chlamydia trachomatis* and can be used as a starting point to develop new drugs selective toward this pathogen.

RESULTS AND DISCUSSION

Chemistry. Our synthetic strategy was based on reacting a substituted sulfonyl aryl carboxylic acids with the desired amine.[35,41] The carboxylic acid derivatives (**7a−7f**, Scheme 1)

Scheme 1. Synthesis of Key Carboxylic Acid Intermediates 7a−7f[a]

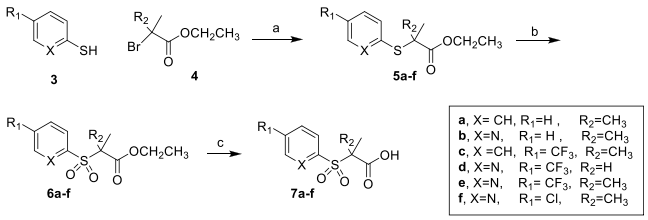

[a]Reagents and conditions: (a) KOH, EtOH, reflux, 18 h; (b) oxone, dioxane−water (5:1), 23 °C, 18 h; (c) LiOH·H_2O, THF−water (4:1), 23 °C, 18 h.

were prepared by reacting 2-thioaryl derivatives (**3**) with an appropriate α-halo ester derivative (**4**).[35] The obtained thioether derivatives **5a−5f** were reacted, without further purification, with potassium peroxymonosulfate (OXONE) in a dioxane−water mixture to provide the corresponding sulfone derivatives **6a−6f**. Hydrolysis of the ester group under mild basic conditions provides the corresponding carboxylic acid derivatives **7a−7f**. The monomethyl acid derivative **7d** was alternatively prepared, in two steps, by the reaction of 5-(trifluoromethyl)pyridine-2-thiol with 2-bromopropanoic acid followed by oxidation (Scheme S1).[46]

The carboxylic acid derivatives **7a−7f** were activated using PYBOP and DIPEA in tetrahydrofuran (THF) and then reacted with 3-phenylpropylamine to yield six derivatives, **9−14** (Scheme 2).[41,47,48] All the prepared molecules satisfy the Lipinski rule of five (Table S1).[49] PYBOP proved to be the best choice for this type of reaction while other coupling agents, such as HBTU and HATU (with or without Oxyma),

https://dx.doi.org/10.1021/acs.jmedchem.0c00371
J. Med. Chem. 2020, 63, 4370−4387

Scheme 2. Synthesis of ACP1 Analogues with the Modified Western Part[a]

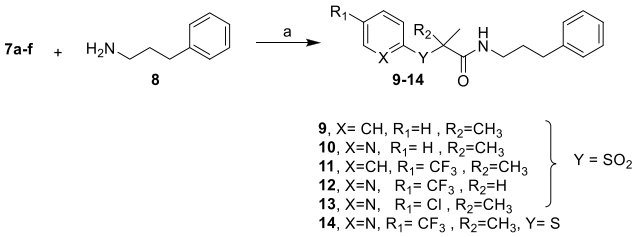

[a]Reagents and conditions: (a) PYBOP, DIPEA, THF, RT, l h.

only gave trace amounts of the product. The selection of THF was also critical because using DMF resulted in a Smiles rearrangement reaction due to the presence of a sulfonyl moiety (Scheme S2).[50]

Then, five derivatives (**16**−**20**, Scheme 3) were synthesized to understand the importance of the thiol and chloro atoms on

Scheme 3. Synthesis of ACP1b Analogues by Modification in the Western Fragment[a]

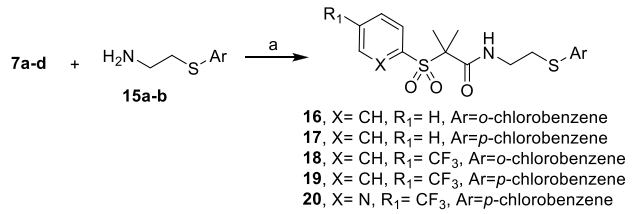

[a]Reagents and conditions: (a) PYBOP, DIPEA, THF, 23 °C, l h.

the eastern part of the molecule. Accordingly, the amine precursors **15a,15b** (**a** = 2-((2-chlorophenyl)thio)ethan-1-amine; **b** = 2-((4-chlorophenyl)thio)ethan-1-amine) were prepared as reported previously (Scheme S4)[51,52] and reacted with the carboxylic acids **7a**−**7d**.

To investigate the importance of the thiol on the eastern part, we synthesized derivatives **23**−**31** (Scheme 4). First, we converted 2-bromoethylamine (**21**) into the functionalized 3-phenoxyethylamines **22a**−**22c** (**a** = 2-phenoxyethan-1-amine; **b** = 2-(2-chlorophenoxy)ethan-1-amine; **c** = 2-(4-chlorophenoxy)ethan-1-amine). These molecules were coupled to the carboxylic acid intermediates **7a**, **7c**, and **7f** using the conditions described above.

To further develop SAR, we synthesized a set of compounds with restricted rotation by including piperazine linkers in the middle part (**33**−**45**). The carboxylic acid derivatives **7d,f** were reacted with various piperazines (**32a**−**32j**) to evaluate the effect of this substitution on the eastern region of the molecules, as shown in Scheme 5. This rigid linker restricts the flexibility of the side chain and reduces the entropic penalty of binding of the compounds to their target.[53,54]

Scheme 5. Synthesis of ACP1 Analogues with a Rigid Linker[a]

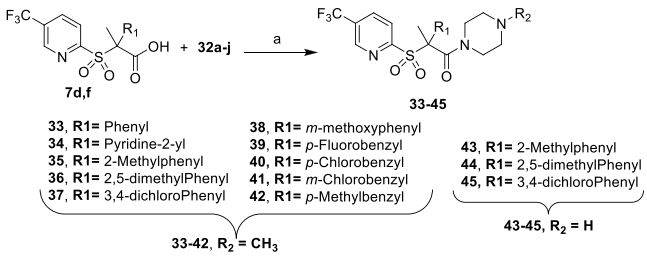

[a]Reagents and conditions: appropriate piperazine derivative, PYBOP, DIPEA, THF, 23 °C, l h.

Biological Evaluation. *Antichlamydial Activity.* As mentioned, once EBs are internalized, they differentiate into RBs and remain within a membrane-bound vesicle called an inclusion. This protects the pathogen during its developmental cycle. Because the inclusions are linked to the growth and replication of the pathogen,[55,56] we determined antichlamydial activity by analyzing the number and size of the inclusions using an immunofluorescence assay (IFA).[57,58] Briefly, HEp-2 cells were infected with *C. trachomatis* serovar L2, and the synthesized molecules were added at 50 μg/mL, 8 h postinfection (hpi). After 16 h (total incubation of the cells for 24 h), the inclusions were analyzed and compared with the control, untreated cells. The morphology and viability of the cells were examined under phase contrast microscopy to ensure the eradication of the inclusions was not the result of a reduction in viable cells due to compound toxicity (Figure 3b and the Supporting Information). Table 1 shows the results of this prescreening assay.

Scheme 4. ACP Derivatives with Oxygen in the Western Part[a]

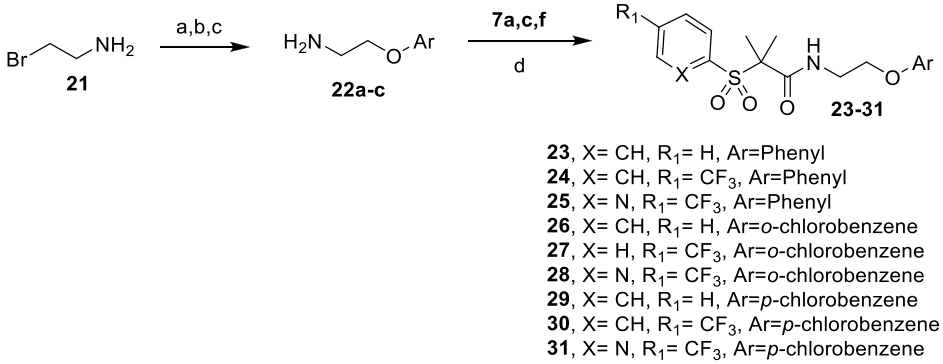

[a]Reagents and conditions: (a) BOC_2O, DCM, 23 °C, overnight; (b) *p*-chlorophenol, K_2CO_3, DMF; (c) TFA, H_2O, dioxane, 23 °C, 18 h; (d) PYBOP, DIPEA, THF, 23 °C l h.

https://dx.doi.org/10.1021/acs.jmedchem.0c00371
J. Med. Chem. 2020, 63, 4370−4387

Table 1. Initial Antichlamydial Activity Screening of ACP Derivatives vs *C. trachomatis* (Serovar LGV-L2)[a]

cmpd no.	inhibition activity	cmpd no.	inhibition activity
ACP1	−	28[59]	+
1	++	29	−
2	−	30	−
9	−	31	−
10	−	33	−
11	++	34	−
12	−	35	+
13	+	36	++
14	toxic	37	++
16	−	38	+
17	−	39	−
18[59]	++	40	++
19	++	41	++
20[59]	−	42	+
23	−	43	−
24[59]	++	44	−
25	++	45	−
26	−		
27	++		

[a]Compounds were tested at 50 μg/mL. The compound's effectiveness is a measure of its ability to inhibit chlamydial inclusions and can be divided into three categories: [−] = not effective; [+] = intermediate effect; [++] = effective. One compound demonstrated clear toxicity to the host cells and is noted.

We found that analogues **9** and **10**, molecules lacking the trifluoromethyl group, were inactive, which highlighted the importance of electron withdrawing groups at position 4. Meanwhile, the presence of the trifluoromethyl-substituent (compound **11**) provided antichlamydial activity. Next, we replaced the trifluoromethyl group with a chlorine atom (**13**), obtaining an analogue with moderate activity. Two other derivatives containing an unsubstituted phenyl group (**16**, **17**) and a chlorine atom on the eastern part of the molecule did not exhibit activity. However, the addition of the trifluoromethyl group, while keeping with the same substitution pattern on the eastern part (**18**, **19**), yielded antichlamydial compounds.

The importance of the trifluoromethyl substituent was further highlighted in derivatives **23**−**29**, which also possess an aryl ether group. Surprisingly, three molecules contained a trifluoromethyl group and were still inactive against *Chlamydia*: compounds **20**, **30**, and **31**. Note that these inactive compounds possess a chlorine atom at the para position on the eastern portion of the molecules. Collectively, these data suggest a detrimental effect of substitution at the para position. To test the importance of the sulfonyl group, a thioether derivative **14** was synthesized by skipping the oxidation step in Scheme 2. The obtained derivative showed prominent host cell toxicity. Compound **12**, which has one methyl group instead of the *gem*-dimethyl group, was found to be inactive.

Next, we decided to replace the amide bond at the middle part of the core molecule with rigid cyclic amine (piperazine) groups to generate a series of derivatives without hydrogen bond donor groups (Table 1 and Table S1). Compounds **33** and **34**, possessing phenyl or pyridyl groups attached to the piperazine moiety, lacked antichlamydial activity. In contrast, replacement of the phenyl group with an *o*-tolyl (**35**), 2,5-dimethyl phenyl (**36**), or 3,4-dichloro phenyl (**37**) enhanced antichlamydial activity. The inclusion of a methyl spacer between the piperazine and the eastern part, gave molecules **38** and **42**, which displayed moderate activity. The fluorinated analogue of **38**, molecule **39**, did not possess activity, but the chlorinated molecule (**40**) was active. Thus, the data suggest that a larger group with electron withdrawing properties is needed. Molecules **41** and **42** possess substituents at the meta position, and once again, the electron withdrawing group enhanced activity. Finally, three derivatives (**43**−**45**) with a monomethyl group in the middle part exhibited no antichlamydial activity.

After the initial assessment of antichlamydial activity, we determined the impact of the most active compounds *in vitro* by determining the number and morphology of infectious units (the EB) and compared their activity against two antibiotics: spectinomycin and penicillin, which are among the FDA approved antibiotics used to treat STDs.[60,61] We understand penicillin is not commonly used to treat *Chlamydia* since it blocks cell division and growth without eradicating the bacteria but we were looking for a comparison against a common drug.[62] HEp-2 cells were infected with *C. trachomatis* serovar L2, and then the selected molecules were added; 50 μg/mL of our compounds, 128 μg/mL of spectinomycin (2× minimum inhibitory concentration. (MIC)),[63] and 5 units/mL of penicillin (3× MIC)[63] 8 h after infection. To accurately determine the "infectious progeny" by quantifying the number of chlamydiae from treated cultures as well as controls, we used an inclusion forming units (IFU) assay as described elsewhere.[62] Briefly, after 24 h, the infected cells were scraped, collected in chlamydia transport medium, and used to reinfect a fresh HEp-2 cell monolayer. The chlamydial infectivity, reported as IFUs, was determined by counting the number of fluorescent inclusions after immunofluorescent staining, 24 h postsecondary infection (Figures 2 and 3a) from a minimum of 15 fields of view using an epifluorescence microscope. We also assessed the morphology, size, and appearance of the chlamydial inclusions after exposure to the tested compounds. Among the designated compounds, derivatives **11**, **24**, **25**, **35**, **37**, **40**, and **41** showed a remarkable impact on chlamydiae.

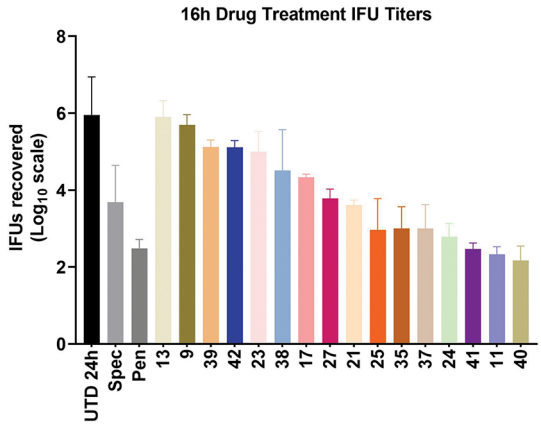

Figure 2. Quantification of chlamydial growth in the presence of selected ACP derivatives (numbered) and antibiotics spectinomycin (Spec) and penicillin (Pen) as compared to an untreated (UTD) control at 24 h postinfection. Results are reported as an average with standard deviation on a $\log_{10}$ scale and represent a minimum of two biological replicates.

https://dx.doi.org/10.1021/acs.jmedchem.0c00371
J. Med. Chem. 2020, 63, 4370−4387

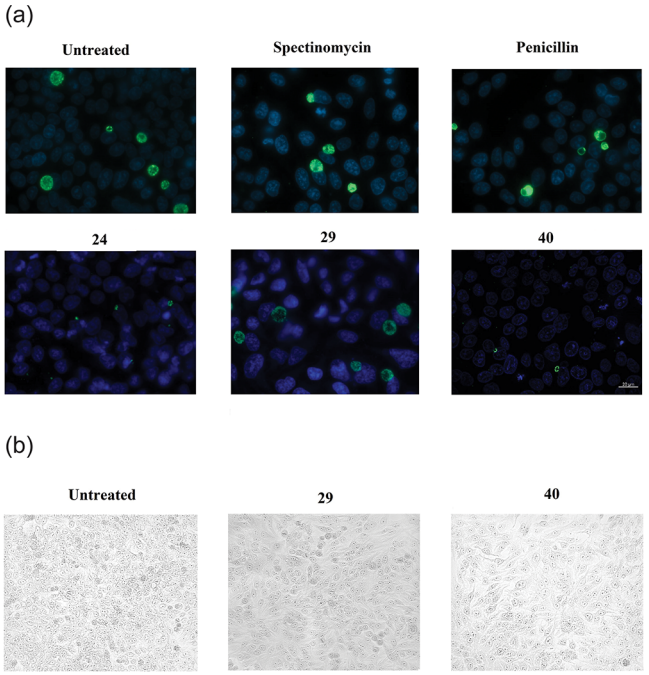

Figure 3. (a) Immunofluorescence images of the effects of selected compounds on chlamydial inclusion growth. In blue, HEp-2 cells nuclei; in green, chlamydial inclusions. Images were acquired at 24 h postinfection. (b) Cell morphology images using an EVOS FL auto cell imaging microscope.

Compound **40** showed superior activity than spectinomycin, which was used at a concentration roughly 2.5-fold higher (128 μg/mL) and on par with penicillin (5 U/mL to ~3 μg/mL).[64] The immunofluorescent staining (Figure 3a) revealed the inclusions were relatively small and irregular in cells treated with our compounds when compared with the untreated sample and the reference molecules. The cell morphology investigation (Figure 3b) supported that the tested compounds did not show any toxicity during the assay. We reasoned the high activity of this derivative is due to the combination of amide bond restriction in the middle part, the electron withdrawing group in the eastern part, and the acceptable log *P* and HBD/HBA values (Table S1).

Dose–Response Curve. The dose–response effect was investigated for compound **40** on *Chlamydia* at six concentrations using the IFU assay described previously. As expected, compound **40** was found to exhibit inhibition activity in a dose-dependent manner with an IC_{50} (the concentration, which shows 50% inclusion inhibition) of 5.2 μg/mL (Figure 4a). The dose–response curve revealed a high reduction of chlamydial progeny in a consistent way (Figure 4a). Besides affecting progeny yields, the immunofluorescence images showed an increase in the number and size of chlamydial inclusions as the concentration of the compound decreased (Figure 4). Compound **40** reduced the chlamydial infection at both 100 and 50 μg/mL and still maintained good activity up to a concentration of 12.5 μg/mL, with inclusion yields around 60% lower than the untreated cells. We did not observe cell toxicity at 100 μg/mL, which supports the tolerability of **40**.

Antichlamydial Effect of ACP Derivatives in Comparison with Two Marketed Drugs. We further tested the activity of compound **40** at 50 μg/mL and 5.20 μg/mL (IC_{50} value) against our lead compound (ACP1b) at 50 μg/mL, and two frontline antibiotics, azithromycin and doxycycline, at their

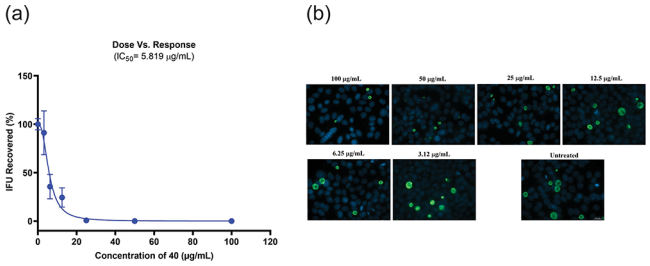

Figure 4. (a) Dose–response curve for the effect of 40 reported on a $\log_{10}$ scale. (b) Immunofluorescence analysis of **40** inhibitory effect. In green, chlamydial inclusions; in blue, HEp-2 cell nuclei.

reported minimal chlamydicidal concentrations (MCCs), (4 μg/mL and at 1 μg/mL, respectively).[65−68] We confirmed our lead compound (ACP1b) and compound **40** showed good inhibitory activity against chlamydiae (Figure 5a). The four

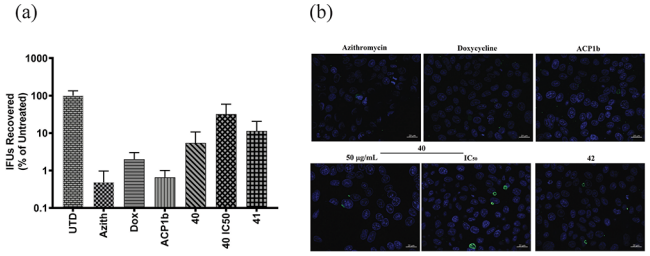

Figure 5. (a) Quantification of chlamydial growth in the presence of selected ACP derivatives (40 and ACP1b) and antibiotics azithromycin (Azith) and doxycycline (Dox) as compared to an untreated (UTD) control at 24 h postinfection. (b) Immunofluorescence analysis of the tested compounds inhibitory effect; in green, chlamydial inclusions; in blue, HEp-2 cells nuclei.

tested compounds elicited a notable impact on the size as well as the number of the inclusions (Figure 5b). Despite the reported treatment efficacy of both drugs,[69] these antibiotics are associated with two major concerns. The first is treatment failure rate, which can reach 22% and lead to repeat infections, and existing complications associated with chlamydial infections.[70] The second concern involves bacterial resistance that can be triggered by these broad spectrum therapies (in both *Chlamydia* and other normal flora bacteria)[71−74] and can lead to chlamydial persistence.[75−77] Given these concerns and the promising activity of our compounds, we consider ACP a new scaffold with a unique mechanism of action that can serve as a starting point to generate new antichlamydial agents.

Mechanism of Action. Antibiotics can be bacteriostatic, stopping growth or reproduction by targeting essential functions such as cell wall growth, or bactericidal, which kills the bacteria.[78] To classify compound **40**, we treated HEp-2 cells at 8 hpi with 50 μg/mL of the molecule, followed by incubation for an additional 16 h. Subsequently, the drug was washed out before the infected cells were further incubated for another 24 h. As seen in Figure 6a, compound **40** reduced the inclusion yield as expected, but 24 h after drug washout, the number of inclusions increased by ~1 log in comparison with untreated cells, suggesting a bacteriostatic mechanism of action. Further, incubation of the infected cells with **40** for 48 h led to higher inclusion output suggesting a loss of the drug activity via metabolic degradation, development of resistance (unlikely on the time frame of the experiment), or an increase on the total number of inclusions at the end of the

https://dx.doi.org/10.1021/acs.jmedchem.0c00371
J. Med. Chem. 2020, 63, 4370−4387

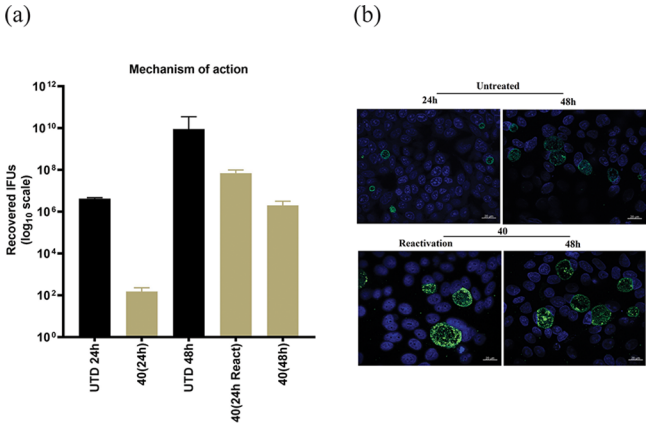

Figure 6. (a) Investigation of the bacteriostatic or bactericidal activity of **40** as measured by IFU output and reported on a $\log_{10}$ scale. (b) Immunofluorescence analysis of **40** impact 24 h after its removal (reactivation) in comparison with untreated (UTD) samples at 24 h postinfection. In green, chlamydial inclusions; in blue, HEp-2 cell nuclei.

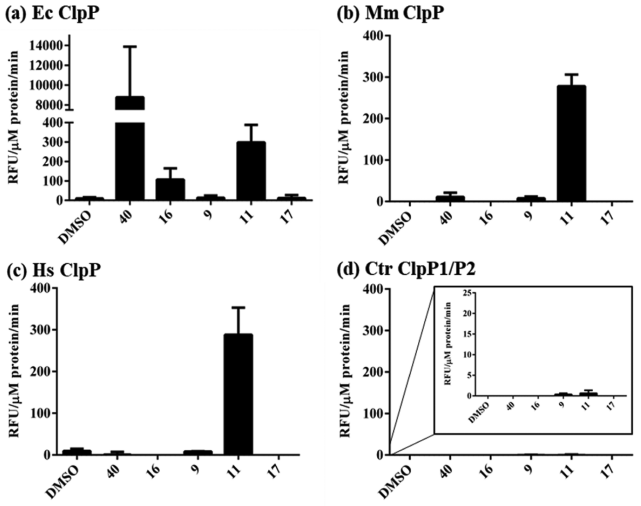

Figure 7. In vitro protease assay shows the degradation of casein (unlabeled) by three different recombinant ClpP preparations with or without the compounds as assessed by SDS-PAGE analysis. Ec = *Escherichia coli*, Ctr = *Chlamydia trachomatis*, Hs = *Homo sapiens*, Mm = *Mus musculus*. DMSO is a negative control. Note the mammalian ClpP orthologues migrate slightly lower than casein in the gels. The top band in all images is casein and the lower band is the respective ClpP. Molecular weight markers (in kDa) are present in lane 1 of each gel.

cycle, which cannot be eradicated by the drug or a combination of the three. Additional studies are needed to understand this result.

Although the EB numbers increased after drug removal or incubation for an additional 24 h, we noticed a reduction in the inclusion size and loss in inclusion morphology, reflecting a lack of development of the pathogen, which suggests the impact of our compounds on chlamydial growth (Figure 6b). Generally, the static effect of these compounds was consistent with a general mechanism depending on inhibition of protein turnover inside the chlamydial organisms. Bacteriostatic drugs can help in treatment of chlamydia infections since the progression of *Chlamydia* into a latent form and the clearance of bacteria are not only dependent on the antibiotic category but also on the capability of the host cells to eliminate the bacteria.[79]

In Vitro Protease Activity. The presented compounds are analogues to known ClpP activators.[41,59] Therefore, we tested the ability of selected compounds to stimulate ClpP-dependent protein degradation *in vitro* in the absence of a AAA+ chaperone. The protease activities of recombinant ClpP1 and ClpP2 from *C. trachomatis* L2, recombinant ClpP from *E. coli*, and recombinant ClpP from human and mouse cells (mitochondrially localized) were measured in the presence and absence of ACPs (Figure 7).[41] Briefly, 20 μM of FITC-labeled casein was incubated with 1 or 0.1 (**40** only) μM ClpP from *E. coli*, 1 μM mammalian ClpP, or 6 μM of *C. trachomatis* ClpP1 and ClpP2 at 32 °C for 3 h with or without compounds. Fluorescence owing to FITC-casein degradation was measured every 3 min. In parallel, degradation of unlabeled casein was also performed and measured by using SDS-PAGE followed by staining with Coomassie Brilliant Blue (Figure S4). Derivatives **11** and **40** enabled some species of ClpP to degrade casein in the absence of a chaperone while little or no degradation was observed for compounds **9**, **16**, or **17**. Importantly, **40** did not activate human or mouse ClpP, suggesting possible selectivity of the compounds for the bacterial ClpP at least in reference to the ClpP from *E. coli*. Surprinsingly, we did not observe activation of chlamydial ClpP1, ClpP2, or the ClpP1/2 dimer (other than some residual decomposition triggered by **9** and **11**). We assessed the activity of the chlamydial ClpP1/P2 preparations using Native PAGE to confirm oligomerization (Figure S2) and digestion of the fluorescent peptide Suc-Luc-Tyr-AMC (Figure S3). This prompted us to consider the killing effect may be the result of ClpP inhibition. However, we did not observe inhibition of ClpP1/P2 activity using the Suc-Luc-Tyr-AMC fluorescent peptide assay. Also, under the conditions tested, we did not observe alterations in ClpP1/P2 activity in the presence of the compounds and the chaperones (data not shown). The results suggest that while *E. coli* ClpP is activated chlamydial ClpP function is not altered, suggesting the molecules may have a mechanism of action independent of this target.

Other Antimicrobial Activity. To evaluate the selectivity of our molecules, we tested their biological activity against other lab strains and ESKAPE microorganisms and selected fungal pathogens: *Staphylococcus aureus* JE 2, *S. aureus* ATCC 43300 MRSA; *E. coli* ATCC 25922; *E. coli* K12, *P. aeruginosa* ATCC 27853; *K. pneumoniae* ATCC 700603; *Acinetobacter baumannii* ATCC 19606; *Candida albicans* ATCC 90028; and *Cryptococcus neoformans* var. grubii H99 ATCC 20882. Notably, none of our compounds showed inhibitory activity against these species in a preliminary screening at 32 μg/mL (Table S2). To further investigate their selectivity, we subjected *S. aureus* JE2 and *E. coli* K12 to concentrations up to 256 μg/mL of compounds **11**, **21**, **25**, **28**, **35**, **37**, **40**, **42**, and once again, bacterial death was not observed. These results indicate that the compounds may be selective for *Chlamydia*. These data also suggest the molecules may not affect the normal gut flora, which in turn suggests the development of widespread resistance is unlikely. We think the lack of activity against other microorganisms is due to the unique cell wall structure of *C. trachomatis* when compared to other bacteria and the unique developmental cycle of *Chlamydia*, which may favor the selectivity of the compounds. In support of these points, **40** was a strong activator of the *E. coli* ClpP *in vitro* (Figure 6)

https://dx.doi.org/10.1021/acs.jmedchem.0c00371
J. Med. Chem. 2020, 63, 4370−4387

without showing antibacterial properties toward either tested *E. coli* strain.

Cytotoxicity. The previous assays not only indicated antichlamydial activity but also low toxicity toward the HEp-2 host cells (Figure 5b and Figure S1). To further examine the tolerability of the synthesized compounds, we evaluated their *in vitro* toxicity against epithelial cervix adenocarcinoma (HeLa 229) and human keratinocyte (HaCaT) cells. Molecules were evaluated at a concentration of 50 μg/mL, i.e., the highest tested concentration used in antichlamydial assays, and results are summarized in Figure 8. The compounds were tolerated by HeLa 229 cells (only **20** and **24** presented viabilities less than 65%), while the normal HaCaT proved to be more sensitive to some of the molecules. For example, compound **40** was not toxic toward HeLa 229 cells but affected ~50% of the HaCaT cells. Compounds **24**, **37**, and **42** were more tolerated by the HaCaT cells. This result is not necessarily consistent with the *in vitro* casein degradation data. For example, **11** presented toxicity toward both cells and activated mammalian ClpP but **40** did not activate these ClpP orthologues. Future studies will be performed to assess if the observed degradation data is related to a limit of detection issue with the casein assay in combination with an increased need for ClpP/mitochondrial function in the HaCaT cells versus the HeLa cells or to other off-target mechanisms of action.

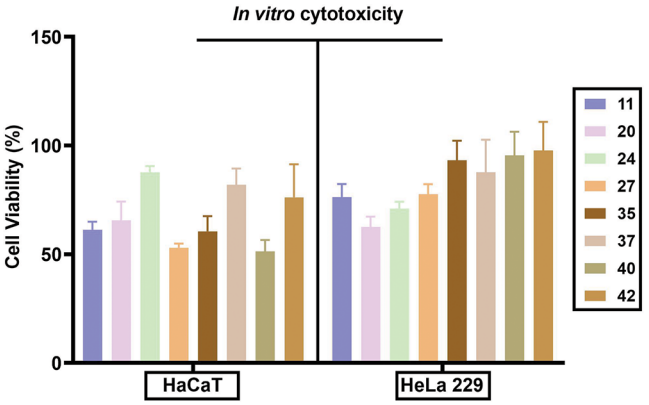

Figure 8. Toxicity analysis of the most active compounds against HeLa 229 and human keratinocytes.

Mutagenic Studies. One major concern of potential antibiotics is their mutagenesis potential, which can damage the host cells and facilitate the adaptation of the bacteria to the antibiotic pressure and other types of stress. Accordingly, we evaluated whether the ACP derivatives were mutagenic toward eukaryotes using the Somatic Mutation and Recombination Tests (SMART) in wing-somatic cells of *Drosophila melanogaster*.[80] This *in vivo* assay simultaneously detects mutational and mitotic recombination events and quantifies the recombinogenic activity of chemicals and drugs. Some antimicrobial drugs have been reported to promote DNA damage because of oxidative stress in the mammalian genome,[81−83] leading to severe side effects such as bone marrow depression, aplastic anemia, and leukemia. We analyzed marked trans-heterozygous descendants (*mwh/flr3*) resulting from standard (ST) and high bioactivation (HB)

Table 2. Frequency of Mutant Spots in the Wings of Marked trans-Heterozygous Descendants (*mwh/flr*^{3}) of *D. melanogaster* Using the Standard Cross (ST) and Marked Trans-Heterozygous Descendants (*mwh/flr*^{3}) of *D. melanogaster* Using the High Bioactivation (HB) after Chronic Treatment of Larvae with 11, 40, and 41 Derivatives

			spots per fly (no. of spots) statistical diagnosis[a]				
cmpd ID	concn (mM)	no. of flies (N)	small single spots (1−2 cell)[b] $m = 2$	large single spots (>2 cell)[b] $m = 2$	twin spots $m = 5$	total spots $m = 2$	spots with *mwh clone*[c] (n)
			mwh/flr^3 of *D. melanogaster*−Standard Cross (ST)				
	control	20	0.40 (8)	0.15 (3)	0.0 (0)	0.55 (11)	10
	0.25	20	0.25 (5) −	0.0 (0) −	0.0 (0) −	0.25 (5) −	5
11	0.50	20	0.20 (4) −	0.0 (0) −	0.0 (0) −	0.20 (4) −	4
	1.00	20	0.35 (7) −	0.05 (1) −	0.0 (0) −	0.40 (8) −	8
	0.25	20	0.20 (4) −	0.0 (0) −	0.0 (0) −	0.20 (4) −	4
40	0.50	20	0.15 (3) −	0.0 (0) −	0.0 (0) −	0.15 (3) −	3
	1.00	20	0.30 (6) −	0.05 (1) −	0.0 (0) −	0.35 (7) −	7
	0.25	20	0.10 (2) −	0.05 (1) −	0.0 (0) −	0.15 (3) −	3
41	0.50	20	0.15 (3) −	0.15 (3) −	0.05 (1) −	0.35 (7) −	7
	1.00	20	0.20 (4) −	0.05 (1) −	0.0 (0) −	0.25 (5) −	5
			mwh/flr^3 of *D. melanogaster*−High Bioactivation (HB) Cross				
	control	20	0.25 (5)	0.10 (2)	0.05 (1)	0.40 (8)	8
	0.25	20	0.15 (3) −	0.05 (1) −	0.05 (1) −	0.25 (5) −	5
11	0.50	20	0.10 (2) −	0.15 (3) −	0.0 (0) −	0.25 (5) −	5
	1.00	20	0.20 (4) −	0.05 (1) −	0.05 (1) −	0.30 (6) −	6
	0.25	20	0.45 (9) i	0.0 (0) −	0.0 (0) −	0.45 (9) −	9
40	0.50	20	0.25 (5) −	0.0 (0) −	0.10 (2) −	0.35 (7) −	7
	1.00	20	0.50 (10) i	0.05 (1) −	0.05 (1) −	0.60 (12) −	12
	0.25	20	0.40 (8) −	0.05 (1) −	0.0 (0) −	0.45 (9) −	9
41	0.50	20	0.40 (8) −	0.05 (1) −	0.05 (1) −	0.50 (10) −	10
	1.00	20	0.35 (7) −	0.10 (2) −	0.0 (0) −	0.45 (9) −	9

[a]Statistical diagnoses according to Frei and Würgler [1988]. U test, two-sided; probability levels: −, negative; + , positive; i, inconclusive; $P < 0.05$ vs untreated control. [b]Including *flr*^{3} single spots. [c]Considering *mwh* clones from *mwh* single and twin spots.

https://dx.doi.org/10.1021/acs.jmedchem.0c00371
J. Med. Chem. 2020, 63, 4370−4387

crossings, which were chronically exposed to ACP derivatives at three different concentrations. The frequency of different mutant clones was scored and the total spots, which indicate the final genotoxicity of each compound at different concentrations, are shown in Table 2 and Table S3.

We found that flies treated with **11**, **20**, **24**, **26**, **40**, and **41** displayed frequencies of clone formation (per individual) for the ST and HB crosses ranging from 0.15 to 0.45 ($P < 0.05$) and 0.20 to 0.60 ($P < 0.05$), respectively, at 0.25, 0.5, and 1 mM. The flies treated with compound **26** at 1 mM showed a higher mutation frequency of 0.70 and 0.75 in descendants from both crossings, although these were not statistically significant. Overall, the results were negative, indicating that the compounds are nongenotoxic in somatic cells of *D. melanogaster* at the concentrations tested, even in HB cross, which has high metabolic bioactivation. However, **26** indicated that the mutant spot frequencies are directly dependent on the concentration, and it is possible that concentrations higher than 1 mM may present mutagenic potential. Compounds **11**, **20**, **24**, **26**, **40**, and **41** did not show toxicity against *D. melanogaster* at the tested concentrations, and it was observed that the survival rate in the treated groups did not differ statistically from the negative control ($P < 0.05$).

Stability Studies. We investigated the *in vitro* metabolic stability of the compounds using liver microsomes and mouse plasma. The incubation with human liver microsomes (HLM) is considered a relevant pharmacokinetic indicator for a compound *in vivo*.[84,85] The metabolic half-life ($t_{1/2}$) and the intrinsic clearance (CL_{int}) of compounds **11**, **24**, **25**, **37**, and **40** are summarized in Table 3. The assay revealed that all tested compounds underwent rapid modification with approximately 90% of the drug modified in 10 min as shown in Figure 9. All tested compounds were stable in the negative control experiment (without NADPH) up to 60 min. For compound **40** the main metabolite presented a M + 16 peak (Figure S5), which may correspond to the *N*-oxidated adduct. Fragmentation spectra of both neat and 10 min incubated samples indicated no chemical change in the eastern part (Figure S5). This compound persisted 60 min postincubation with HLM. The metabolic site and the complete chemical structure of this metabolite is still under investigation.

Table 3. *In Vitro* Experimental Values of $T_{1/2}$, Intrinsic Clearance, and Hepatic Clearance[a]

	$T_{1/2}$ (min)		CL(int) μL/(min*mg protein)		CL(int,H) mL/(min*kg body wt)	
cmpd ID	mean	SD	mean	SD	mean	SD
11	6.13	0.16	113.09	3.02	890.58	23.77
24	2.98	0.17	233.77	13.74	1840.91	108.17
25	3.73	0.03	185.60	1.72	1461.60	13.51
37	6.25	0.16	111.96	2.85	873.80	22.45
40	<2.00	NA	NA		NA	

[a]NA: Not applicable

Then, we explored the stability of some representative compounds in mouse plasma and simulated gastric fluid (SGF, pH 1.2) by calculating the percentage of drug remaining after contact with both media. The tested compounds were incubated with diluted mouse plasma and SGF at 37 °C and the samples were analyzed by HPLC−MS. As shown in Figure 10, all the tested compounds exhibited a high stability profile and their concentrations remained constant for up to 120 min. No modification or degradation was detected after the different incubation periods.

CONCLUSION

Caseinolytic protease P (ClpP) activators have been shown to eradicate bacteria and prevent bacterial resistance. *C. trachomatis* is among the few bacterial species that possess two caseinolytic protease paralogues, ClpP1 and ClpP2.[41] The Clp protein machinery system is essential for the chlamydial developmental cycle, which includes differentiation between the EB and RB forms.[86] In this study, we synthesized compounds based on known ClpP activators to kill *C. trachomatis*. We found some interesting lead compounds that were able to eradicate the pathogen. The biological results allowed us to conduct initial SAR studies to identify key regions that promote biological action (Figure 11). Noteworthy is the fact that compounds did not present activity against other types of bacteria, suggesting a degree of selectivity for *Chlamydia*. While the active compounds were able to activate the *E. coli* ClpP, activation of chlamydial ClpP1/2 was not observed as determined by diverse assays. This suggests the compounds may impact *Chlamydia* by affecting a different target. *In vitro* metabolic stability assays revealed these ACP derivatives were enzymatically transformed by liver microsomes in the first 10 min of incubation. Conversely, the compounds demonstrated good stability in mouse plasma and simulated gastric fluid. Our results indicate the ACP derivatives represent a promising scaffold that can be further developed to obtain a specific treatment for *C. trachomatis* infection. Studies are currently underway to understand the target of the molecules.

EXPERIMENTAL PROCEDURES

Chemistry. *General.* All reagents and solvents were used as received from commercial suppliers unless otherwise noted. All used solvents were dried and stored with activated molecular sieves to ensure dryness on the long run. All coupling reactions were carried out in dried glassware under N_2 atmosphere. Reaction progression was detected using thin layer chromatography (TLC), which was performed on Merck silica gel IB2-F plates (0.25 mm thickness), and the spots detected using a UV light source at 254 nm. ^{1}H and ^{13}CNMR spectra were run at 500 MHz in deuterated chloroform ($CDCl_3$) or dimethyl sulfoxide (DMSO-d_6) on a Bruker-500 NMR spectrometer. Chemical shifts are given in parts per million (ppm) on the delta (δ) scale. Chemical shifts were calibrated relative to those of the solvents. Flash chromatography was performed on the RF 200i Flash Chromatography System from Teledyne ISCO. Low-resolution mass spectra were obtained on an Agilent 6120 or 6150 mass spectrometer with an electrospray ionization (ESI) source. High-resolution mass spectra were run using a Q Exactive HF Hybrid Quadrupole Orbitrap mass spectrometer. The tested compounds possessed purities above 95%. The purity tests were performed on an Agilent 1200 HPLC system equipped with a multiple wavelength absorbance UV detector set for 254 nM and using 5 mM C-18 reversed-phase column with methanol and water as a mobile phase. All reported yields refer to isolated compounds. Marvin was used for characterizing of the physicochemical characters of the synthesized compounds, Marvin 20.4, ChemAxon (https://www.chemaxon.com).

General Procedure for the Synthesis of Acid Derivatives 7a−7f. *2-(Arylthio)propanoate Derivatives 5a−5f.* To a stirred solution of an appropriated aryl thiol **3** (3.00 mmol) in ethanol (10 mL) were added potassium hydroxide pellets (0.25 g, 4.40 mmol) followed by ethyl α-bromo ester **4** (3.00 mmol), and the reaction mixture was heated at reflux for 18 h. After completion of the reaction, the flask content was allowed to cool down to room temperature, and the formed inorganic salt was removed by filtration and washed with

https://dx.doi.org/10.1021/acs.jmedchem.0c00371
J. Med. Chem. 2020, 63, 4370−4387

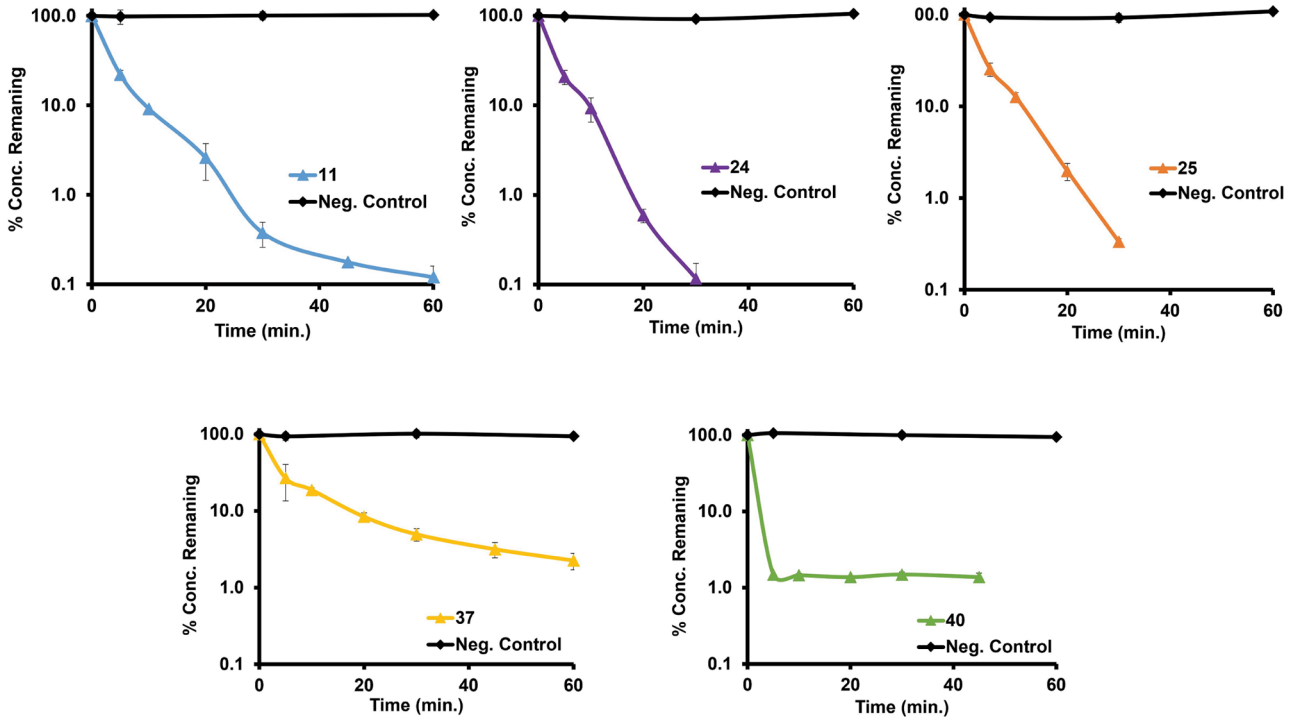

Figure 9. Time-dependent metabolic stability of the tested compounds in human liver microsomes fortified with NADPH and without NADPH (negative control). Metabolic elimination profiles (% turnover or amount remaining vs incubation time). Data shown as mean ± SD (n = 3).

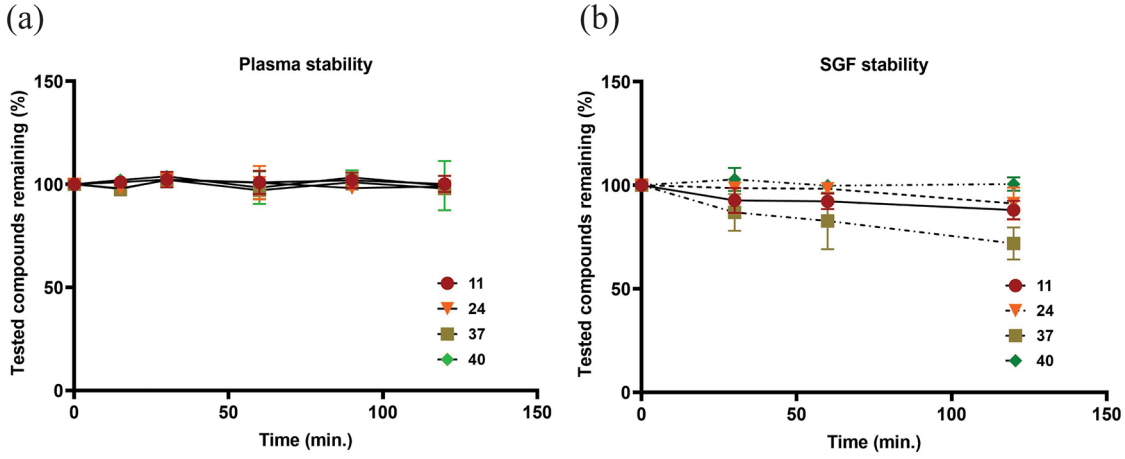

Figure 10. Stability profile in mouse plasma (a) and simulated gastric fluid (b). Relative concentration is represented as a function of incubation time between the tested compound and mouse plasma and simulated gastric fluid (SGF, pH 1.2). Error bars represent SD of three independent experiments.

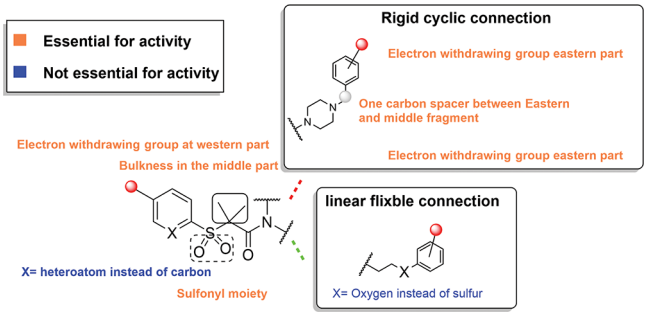

Figure 11. SAR graphical summary.

cold ethanol. The filtrate was evaporated under reduced pressure, and the oily residue was dissolved in DCM (20 mL) and washed with deionized water (3 × 10 mL) and brine solution (1 × 10 mL), dried over anhydrous Na_2SO_4, filtered, and concentrated under reduced pressure to afford the desired product as yellow oil which was used in the next step without further purification.

2-(Arylsulfonyl)propanoate Derivatives ***6a−6f.*** Potassium mono persulfate (OXONE) (2.2 equiv) was added in one portion to a solution of the 2-(arylthio)propanoate derivatives **5a−5f** (3.4 mmol) in dioxane−water 5:1 (25 mL). The formed white suspension was vigorously stirred at 23 °C for 18 h. The white solid was filtered off and washed with dioxane, and the combined filtrate was concentrated under reduced pressure to remove the organic layer. The resulting aqueous solution was extracted with DCM (3 × 15 mL). The combined organic solution was dried over Na_2SO_4 and filtered, and the organic solvent was removed under reduced pressure to afford the desired product as white solids which were used directly in the next step without further purification.

https://dx.doi.org/10.1021/acs.jmedchem.0c00371
J. Med. Chem. 2020, 63, 4370−4387

*2-(Arylsulfonyl) Acid Derivatives **7a−7f**.* 2-(Arylsulfonyl)-propanoate derivative **6a−6f** (3.6 mmol) was dissolved in a mixture of THF−water (4:1, 20 mL), lithium hydroxide monohydrate (7.2 mmol) was milled and added portion wise over 30 min, and the reaction was stirred at room temperature for 18 h. The organic solvent was evaporated under reduced pressure, and the aqueous solution was washed with DCM (1 × 20 mL) to remove byproducts. Then, the aqueous layer was cooled in an ice bath and treated with 1 N HCl to pH 2. The formed precipitate was filtered off to afford the desired products. The physical characters and the spectral data of separated product are listed below.

*2-Methyl-2-(phenylsulfonyl)propanoic Acid (**7a**).* Starting with **6a** (925 mg), white solid (520 mg, 77%). ^{1}H NMR (500 MHz, $CDCl_3$) δ 7.89 (d, J = 7.0 Hz, 2H), 7.71−7.68 (m, 2H), 7.70 (t, J = 7.5 Hz, 1H), 1.63 (s, 6H).

*2-Methyl-2-(pyridin-2-ylsulfonyl)propanoic Acid (**7b**).* Starting with **6b** (925 mg), white solid (280 mg, 41%). ^{1}H NMR (500 MHz, $CDCl_3$) δ 8.77 (m, 1H), 8.14 (d, J = 8.0 Hz, 1H), 8.03 (t, J = 8.0 Hz, 1H), 7.63−7.61 (m, 1H), 1.70 (s, 6H).

*2-Methyl-2-((4-(trifluoromethyl)phenyl)sulfonyl)propanoic Acid (**7c**).* Starting with **6c** (1160 mg), white solid (840 mg, 82%). ^{1}H NMR (500 MHz, $CDCl_3$) δ 8.04 (d, J = 8.5 Hz, 2H), 7.83 (d, J = 8.5 Hz, 2H), 1.66 (s, 6H); ^{19}F NMR δ −63.27 (s).

*2-((5-(Trifluoromethyl)pyridin-2-yl)sulfonyl)propanoic Acid (**7d**).* Starting with **6d** (1120 mg), white solid (750 mg, 85%). ^{1}H NMR (500 MHz, $CDCl_3$) δ 9.01 (s, 1H), 8.253−8.250 (m, 1H), 4.75 (q, J = 7.5 Hz, 1H), 1.74 (d, J = 7.5 Hz, 3H).^{19}F NMR δ −62.45 (s).

*2-Methyl-2-((5-(trifluoromethyl)pyridin-2-yl)sulfonyl)propanoic Acid (**7e**).* Starting with **6e** (1170 mg), white fluffy solid (890 mg, 83%). ^{1}H NMR (500 MHz, $CDCl_3$) δ 9.02 (s, 1H), 8.27−8.22 (m, 2H), 1.76 (s, 6H). ^{19}F NMR δ −62.68 (s).

*2-((5-Chloropyridin-2-yl)sulfonyl)-2-methylpropanoic Acid (**7f**).* Starting with **6f** (1050 mg), white solid (700 mg, 79%). ^{1}H NMR (500 MHz, $CDCl_3$) δ 8.73−8.72 (m, 1H), 8.07 (d, J = 8.5 Hz, 1H), 7.97−7.95 (m, 1H), 1.71 (s, 6H).

General Procedures for Synthesis of 2-Methyl-*N*-(3-phenylpropyl)-2 (arylsulfonyl) Propanamide (9−14). A solution of 2-methyl-2-(arylsulfonyl)propanoic acid **7a−7f** (0.16−0.17 mmol) in dry THF (10 mL) was treated with a solution of PyBOP (87 mg, 0.17 mmol) in THF (1 mL) followed by DIPEA (83 μL). Then, the reaction mixture was stirred at room temperature for 10 min. A solution of the 3-phenylpropan-1-amine (0.16 mmol) in THF (1 mL) was then added dropwise. The formed yellow solution was stirred at room temperature for 1 h. The solvent was removed under vacuum, and the crude product was absorbed onto silica gel and purified by flash column chromatography eluting with a 0−100% gradient of EtOAc in hexanes. The physical characters and the spectral data of the obtained products are listed below.

*2-Methyl-N-(3-Phenylpropyl)-2-(phenylsulfonyl)propanamide (**9**).* Starting with **7a** (37 mg), white solid (46 mg, 84%). ^{1}H NMR (500 MHz, $CDCl_3$) δ 7. 81 (d, J = 7.5 Hz, 2H), 7.65 (t, J = 7.5 Hz, 1H), 7.52 (t, J = 7.5 Hz, 2H), 7.31−7.26 (m, 2H), 7.21−7.18 (m, 3H), 7.05 (br s, 1H), 3.33 (q, J = 6.5 Hz, 2H), 2.70 (t, J = 6.5 Hz, 2H), 1.90 (q, J = 6.5 Hz, 2H), 1.54 (s, 6H). ^{13}C NMR (125 MHz, $CDCl_3$) δ 167.44, 141.18, 135.10, 134.34, 130.04, 129.03, 128.54, 128.40, 126.10, 68.01, 39.90, 33.19, 30.79, 20.93. HPLC purity, 97.1%. HRMS (m/z): $[M + H]^+$ calcd for $C_{19}H_{24}NO_3S$, 346.1399; found, 346.1470; exact mass (monoisotopic) from spectrum, 345.1397.

*2-Methyl-N-(3-Phenylpropyl)-2-(pyridin-2-ylsulfonyl)-propanamide (**10**).* Starting with **7b** (37 mg), white solid (46 mg, 83%). ^{1}H NMR (500 MHz, $CDCl_3$) δ 8.66−8.65 (m, 1H), 8.03 (d, J = 7.5 Hz, 1H), 7.92(t, J = 7.5 Hz, 1H), 7.53−7.51 (m, 1H), 7.29−7.26 (m, 1H), 7.19−7.18 (m, 4H), 3.33 (q, J = 6.5 Hz, 2H), 2.70 (t, J = 6.5 Hz, 2H), 1.91 (q, J = 7.5 Hz, 2H), 1.60 (s, 6H). ^{13}C NMR (125 MHz, $CDCl_3$) δ 167.76, 154.89, 150.25, 141.44, 137.94, 128.47, 128.42, 127.76, 125.99, 124.71, 67.40, 39.94, 33.13, 30.65, 20.73. HPLC purity, 98.9%. HRMS (m/z): $[M + H]^+$ calcd for $C_{18}H_{22}N_2O_3S$, 347.1351; found, 347.1423; exact mass (monoisotopic) from spectrum, 346.1350.

2-Methyl-N-(3-Phenylpropyl)-2-((4-(trifluoromethyl)phenyl)-sulfonyl)propanamide (11). Starting with 7c (48 mg), white solid (53 mg, 81%). ^{1}H NMR (500 MHz, $CDCl_3$) δ 7.94 (d, J = 8 Hz, 2H), 7.78 (d, J = 8.5 Hz, 2H), 7.32−7.29 (m, 2H), 7.22−7.20 (m, 3H), 6.87 (br s, 1H), 3.33 (q, J = 6.5 Hz, 2H), 2.71 (t, J = 6.5 Hz, 2H), 1.93 (q, J = 6.5 Hz, 2H), 1.55 (s, 6H); ^{13}C NMR (125 MHz, $CDCl_3$) δ 166.94, 141.03, 138.7, 136.06, 135.80, 130.68, 128.60, 128.37, 126.11(q, J = 3.75 Hz), 126.19, 121.93, 68.32, 40.02, 33.19, 30.71, 20.67. HPLC purity, 97.4%. HRMS (m/z): $[M + H]^+$ calcd for $C_{20}H_{22}F_3NO_3S$, 414.1272; found, 414.1345, exact mass-(monoisotopic) from spectrum, 413.1727.

*N-(3-Phenylpropyl)-2-((5-(trifluoromethyl)pyridin-2-yl)sulfonyl)-propanamide (**12**).* Starting with **7d** (50 mg), white solid (48 mg, 68%). ^{1}H NMR (500 MHz, $CDCl_3$) δ: 8.97 (s, 1 H), 8.19 (s, 2H), 7.30−7.26 (m, 2H), 7.21−7.16 (m, 3H), 6.58 (br s, 1H), 4.33 (q, J = 7.5 Hz, 1H), 3.32−3.28 (m, 2H), 2.66 (t, J = 7.5 Hz, 2H), 1.85 (p, J = 7.5 Hz, 2H), 1.55 (d, J = 7.0 Hz, 3H). ^{13}C NMR (125 MHz, $CDCl_3$) δ 163.62, 158.79, 147.39, 147.36, 141.13, 135.81, 135.78, 130.22, 128.53, 128.35, 126.12, 123.22, 121.28, 62.55, 39.84, 33.02, 30.70, 11.47. HPLC purity, 98.3. ESIMS calcd for $C_{18}H_{19}F_3N_2O_3S$: 401.42 $[M + H]^+$; found, 401.01. HRMS (m/z): $[M + H]$ calcd for $C_{18}H_{19}F_3N_2O_3S$, 401.1068; found, 401.1139; exact mass (monoisotopic) from spectrum, 400.1067.

Alternative Method for the Synthesis of Molecule 12. *N-(3-Phenylpropyl)-2-((5-(trifluoromethyl)pyridin-2-yl)thio)-propanamide.* To a solution of 2-((5-(trifluoromethyl)pyridin-2-yl)thio)propanoic acid (0.05 g, 0.20 mmol) in dry THF (7 mL), PYBOP (0.08 g, 0.18 mmol) and DIPEA (70 μL, 0.5 mmol) were added and the mixture was stirred at room temperature for 15 min; phenyl propylamine (28 μL, 0.20 mmol) was added. The reaction mixture was stirred at room temperature for 1 h; thereafter, the organic solvent was evaporated under reduced pressure and the crude residue was purified by flash column chromatography to yield the desired product as yellow oil (55 mg, 75%). ^{1}H NMR (500 MHz, $CDCl_3$) δ: 8.69 (s, 1 H), 7.73 (d, J = 8.5 Hz, 1H), 7.29 (d, J = 8.5 Hz, 1H), 7.28−7.24 (m, 2H), 7.19−7.16 (m, 1H), 7.08−7.06 (m, 2H), 4.47 (q, J = 7.5 Hz, 1H), 3.34−3.22 (m, 2H), 2.54 (t, J = 7.5 Hz, 2H), 1.82−1.76 (m, 2H), 1.60 (d, J = 7.5 Hz, 3H).

*N-(3-Phenylpropyl)-2-((5-(trifluoromethyl)pyridin-2-yl)sulfonyl)-propanamide (**12**).* To a stirred solution of 3-phenylpropyl 2-((5-(trifluoromethyl)pyridin-2-yl) thio) propanoate (55 mg, 0.15 mmol) in dioxane/water (5:1, 3 mL) in a 10 mL scintillation vial, in one portion (160 mg, 0.3 mmol), potassium mono persulfate (OXON) was added. The obtained white suspension was stirred at room temperature for 16 h. After the reaction was completed as seen by TLC, the white solid was filtered off, and dioxane was removed under reduced pressure. Then, the aqueous solution was extracted with DCM (3 × 5 mL). The collected organic layers were dried over sodium sulfate, removed under reduced pressure, and purified with flash column chromatography to afford the desired oxidized derivative as white crystals (33 mg, 56%).

*2-((5-Chloropyridin-2-yl)sulfonyl)-2-methyl-N-(3-phenylpropyl)-propanamide (**13**).* Starting with **6f** (42 mg), white solid (55 mg, 88%). ^{1}H NMR (500 MHz, $CDCl_3$) δ 8.58 (s, 1H), 7.97 (d, J = 8.5 Hz, 1H), 7.88−7.86 (dd, J = 8.5 Hz, J = 1.5 Hz, 1H), 7.29−7.26 (m, 2H), 7.20−7.17 (m, 3H), 7.04 (br s, 1H), 3.30 (q, J = 6.5 Hz, 2H), 2.69 (t, J = 7.5 Hz, 2H), 1.90 (q, J = 7.5 Hz, 2H), 1.59 (6H, s). ^{13}C NMR (125 MHz, $CDCl_3$) δ 167.46, 152.64, 149.31, 141.33, 137.51, 137.03, 128.52, 128.40, 126.06, 125.70, 67.65, 39.98, 33.12, 30.60, 20.62. HPLC purity, 98.5%. HRMS (m/z): $[M + H]^+$ calcd for $C_{18}H_{21}ClN_2O_3S$, 381.0961; found, 381.1033; exact mass (monoisotopic) from spectrum, 380.0960.

*2-Methyl-N-(3-phenylpropyl)-2-((5-(trifluoromethyl)pyridin-2-yl)-thio)propanamide (**14**).* Starting with thioacid (50 mg), white solid (47 mg, 76%). ^{1}H NMR (500 MHz, $CDCl_3$) δ 8.65 (s, 1H), 7.71 (d, J = 8.5 Hz, 1H), 7.34 (br s, 1H), 7.29 (d, J = 8.5 Hz, 1H), 7.24 (t, J = 7.5 Hz, 2H), 7.16 (t, J = 7.5 Hz, 1H), 7.06 (d, J = 7.5 Hz, 2H), 3.26 (q, J = 7.5 Hz, 2H), 2.54 (t, J = 6.5 Hz, 2H), 1.76 (q, J = 7.5 Hz, 2H), 1.68 (s, 6H). ^{13}C NMR (125 MHz, $CDCl_3$) δ 173.85, 162.41, 146.06, 146.01, 141.36, 133.14, 133.11, 128.43, 128.24, 125.97, 124.59,

https://dx.doi.org/10.1021/acs.jmedchem.0c00371
J. Med. Chem. 2020, 63, 4370−4387

123.39, 123.12, 122.85, 52.77, 39.59, 33.13, 30.91, 26.61. HPLC purity, 98.9%. HRMS (m/z): $[M + H]^+$ calcd for $C_{19}H_{21}F_3N_2OS$, 383.1327; found, 383.1397; exact mass (monoisotopic) from spectrum, 382.1324. Note: For this derivative, we hydrolyzed 100 mg of **5e** using the same condition, followed by the reaction with phenyl propylamine.

General Procedures for Synthesis of 2-((Chlorophenyl)-thio]ethan-1-amine (15a, 15b)..[51,52] To a solution of sodium metal (97.0 mg, 4.22 mmol) in *i*-PrOH (15 mL), an appropriate chlorothiophenol derivative (475 mg, 3.30 mmol) was added, and the reaction mixture was stirred at room temperature for 30 min. Then, 2-oxazolidinone (100 mg, 1.14 mmol) was added and the reaction was heated at reflux for 6 h. After reaction completion, the organic solvent was evaporated under vacuum, and the crude product was purified using flash column chromatography (DCM−methanol 90:10) to afford the desired product as the following.

*2-((2-Chlorophenyl)thio)ethan-1-amine (**15a**).* Colorless oil with fruity odor (125 mg, 36%). ^{1}H NMR (500 MHz, $CDCl_3$) δ: 7.38−7.31 (dd, J = 7.0 Hz, 1H 2H), 7.22−7.18 (m, 1H), 7.13−7.10 (m, 1H), 3.03 (t, J = 6.0 Hz, 2H), 2.94 (t, J = 6.0 Hz, 2H), 1.70 (s, 2H).

*2-((4-Chlorophenyl)thio)ethan-1-amine (**15b**).* Yellow oil with characteristic odor (305 mg, 88.6%). ^{1}H NMR (500 MHz, $CDCl_3$) δ: 7.28 (d, J = 8.5 Hz, 2H), 7.229−7.23 (m,4H), 2.90−2.89 (m, 2H), 1.54 (br s, 2H).

*N-(2-((Chlorophenyl)thio)ethyl)-2-methyl-2-(arylsulfonyl)-propanamide (**16**−**20**).* To a solution of the appropriate carboxylic acid derivative (**7a**−**7e**, 0.16−0.22 mmol) in dry THF (5 mL), PYBOP (1.05 equiv) and DIPEA (2.7 equiv) were added followed by stirring at room temperature for 10 min under nitrogen atmosphere. The reaction mixture was then charged with an appropriate chlorophenyl thioethan-1-amine derivative (**15a**, **15b** 0.16 mmol) and stirred for 1 h, after reaction completion, THF was evaporated under reduced pressure and the crude product was purified by flash column chromatography to yield the desired product.

*N-(2-((2-Chlorophenyl)thio)ethyl)-2-methyl-2-(phenylsulfonyl)-propanamide (**16**).* Starting with **7a** (50 mg) and **15a** (40 mg), white solid (70 mg, 82%). ^{1}H NMR (500 MHz, $CDCl_3$) δ: 7.84 (d, J = 8.0 Hz, 2H), 7.64−7.52 (m, 1H), 7.50−7.44 (m, 2H), 7.44−7.37 (m, 3H include br s peak), 7.23−7.14 (m, 1H), 7.14−7.12 (m, 1H), 3.51 (q, J = 6.5 Hz, 2H), 3.11 (t, J = 6.5 Hz, 2H), 1.55 (s, 6H). ^{13}C NMR (125 MHz, $CDCl_3$) δ 167.91, 135.00, 134.56, 134.41, 134.12, 130.12, 129.99, 129.85, 129.06, 127.43, 68.06, 39.19, 31.95, 20.85. HPLC purity, 95.3%. ESIMS calcd for $C_{18}H_{20}ClNO_3S$: 397.06; found mass $[M + H]^+$, 398.00. HRMS (m/z): $[M + H]^+$ calcd for $C_{18}H_{20}ClNO_3S$, 398.0573; found, 398.0647; exact mass (monoisotopic) from spectrum, 397.0574.

*N-(2-((4-Chlorophenyl)thio)ethyl)-2-methyl-2-(phenylsulfonyl)-propanamide (**17**).* Starting with **7a** (50 mg) and **15b** (40 mg), white solid (67 mg, 77%). ESIMS calcd for $C_{18}H_{20}ClNO_3S$, 397.06; found mass $[M + H]$: 398.00. ^{1}H NMR (500 MHz, $CDCl_3$) δ: 7.85 (d, J = 7.5 Hz, 2H), 7.68 (t, J = 7.5 Hz, 2H), 7.53 (t, J = 8.0 Hz, 2H), 7.40 (br s, 1H), 7.36 (d, J = 9.0 Hz, 2H), 7.29 (d, J = 8.5 Hz, 2H), 3.49 (q, J = 6.5 Hz, 2H), 3.09 (t, J = 6.5 Hz, 2H), 1.56 (s, 6H). ^{13}C NMR (125 MHz, $CDCl_3$) δ 167.85, 134.98, 134.43, 133.30, 132.77, 131.31, 130.08, 129.33, 129.07, 68.03, 39.26, 33.25, 20.87. HPLC purity, 98.7. ESIMS calcd for $C_{18}H_{20}ClNO_3S$: 397.06; found mass $[M + H]^+$: 398.00. HRMS (m/z): $[M + H]^+$ calcd for $C_{18}H_{20}ClNO_3S$, 398.0573; found, 398.0647, exact mass (monoisotopic) from spectrum, 397.0575.

*N-(2-((2-Chlorophenyl)thio)ethyl)-2-methyl-2((4-(trifluoromethyl)phenyl)sulfonyl) Propanamide (**18**).* Starting with **7c** (50 mg) and **15a** (33 mg), white solid (69 mg, 87%). ^{1}H NMR (500 MHz, $CDCl_3$) δ: 7.98 (d, J = 8.0 Hz, 2H), 7.74 (d, J = 8.0 Hz, 2H), 7.43−7.38 (m, 2H), 7.30 (br s, 1H), 7.26−7.22 (m, 1H), 7.18−7.14. (m, 1H), 3.51 (q, J = 6.5 Hz, 2H), 3.12 (t, J = 6.5 Hz, 2H), 1.57 (s, 6H). ^{13}C NMR (DMSO-d_6) δ 167.46, 138.69, 134.85, 133.86, 130.78, 130.18, 130.09, 127.47, 126.15, 126.12, 68.35, 39.13, 32.27, 20.65. HPLC purity, 97%. HRMS (m/z): $[M + H]^+$ calcd for $C_{19}H_{19}ClF_3NO_3S_2$, 466.0447; found, 466.0522; exact mass (monoisotopic) from spectrum, 465.0449.

*N-(2-((4-Chlorophenyl)thio)ethyl)-2-methyl-2-((4-(trifluoromethyl)phenyl)sulfonyl) Propanamide (**19**).* Starting with **7c** (50 mg) and **15b** (33 mg), white crystals (65 mg, 82%); ^{1}H NMR (500 MHz, $CDCl_3$) δ: 7.96 (d, J = 8.0 Hz, 2H), 7.77 (d, J = 8.0 Hz, 2H), 7.34 (d, J = 8.5 Hz, 2H), 7.28 (d, J = 8.5 Hz, 2H), 7.24 (br s, 1H), 3.49 (q, J = 6.0 Hz, 2H), 3.08 (t, J = 6.5 Hz, 2H), 1.56 (s, 6H). ^{19}F NMR δ − 63.31 (s). ^{13}C NMR (125 MHz, $CDCl_3$) δ 167.36, 138.64, 135.98 (q, J = 32.5 Hz), 133.14, 132.92, 131.36, 130.74, 129.38, 126.15 (q, J = 3.75 Hz), 124.08, 121.90, 68.32, 39.26, 33.33, 20.65. ^{19}F NMR δ −63.31 (s). HPLC purity, 99.2%. ESIMS calcd for $C_{19}H_{19}ClF_3NO_3S_2$: 465.04; found mass $[M + H]^+$, 466.0. HRMS (m/z): $[M + H]^+$ calcd for $C_{19}H_{19}ClF_3NO_3S_2$, 466.0447; found, 466.0523, exact mass (monoisotopic) from spectrum, 465.0450.

*N-(2-((4-Chlorophenyl)thio)ethyl)-2-methyl-2-)(5-(trifluoromethyl)pyridin-2-yl)sulfonyl) Propanamide (**20**).* Starting with **7e** (50 mg) and **15b** (31 mg), white solid (53 mg, 68%). ^{1}H NMR (500 MHz, $CDCl_3$) δ: 8.91 (s, 1H), 8.21−8.17 (m, 2H), 7.37 (br s, 1H), 7.33 (d, J = 8.5 Hz, 2H), 7.26 (d, J = 8.5 Hz, 2H), 3.48 (q, J = 6.5 Hz, 2H), 3.09 (t, J = 6.5 Hz, 2H), 1.62 (s, 6H). ^{13}C NMR (125 MHz, $CDCl_3$) δ 167.09, 158.12, 147.16, 135.58, 133.44, 132.73, 131.25, 130.45, 130.18, 129.28, 124.47, 121.27, 67.59, 39.47, 33.09, 20.71. HPLC purity, 95%. ESIMS calcd for $C_{19}H_{19}ClF_3NO_3S_2$, 466.04; found mass $[M + H]^+$, 467.19. HRMS (m/z): $[M + H]^+$ calcd for $C_{19}H_{19}ClF_3NO_3S_2$, 467.0447; found, 467.1023.

Synthesis of 2-(4-Chlorophenoxy)ethan-1-amine (22c). Starting from 2-bromo ethan-1-amine **21** (500 mg, 2.45 mmol), the synthesis of **23c** was carried out over three successive steps.

Step 1: Synthesis of tert-butyl (2-Bromoethyl)carbamate. To a stirred solution of 2-bromo ethan-1-amine **21** (500 mg, 2.45 mmol) in DCM (15 mL) was added triethylamine (0.45 mL). The solution was cooled with an ice bath before a solution of di*tert*-butyl dicarbonate (640 mg, 2.9 mmol) in DMC (5 mL) was added dropwise over 15 min. The mixture was stirred at 23 °C for 12 h. After reaction completion (as seen by TLC), the system was quenched with brine (15 mL), the organic layer washed with water (3 × 15 mL), dried over anhydrous Na_2SO_4, and evaporated under reduced pressure to afford the *N*-protected molecule as a yellowish oil (480 mg, 52%) ^{1}H NMR (500 MHz, $CDCl_3$) δ: 5.01 (br s, 1H), 3.50−3.41 (m, 2H), 3.42 (t, J = 5.5 Hz, 2H), 1.41 (s, 12H).

Step 2: Synthesis of tert-butyl (2-(4-Chlorophenoxy)ethyl)-carbamate. *p*-Chlorophenol (250 mg, 1.95 mmol) in DMF (1 mL) was added gradually to a stirred solution of *tert*-butyl (2-bromoethyl) carbamate (300 mg, 1.33 mmol) followed by oven-dried potassium carbonate (280 mg, 2.0 mmol) in DMF (3 mL). The mixture was stirred at 23 °C for 24 h before the flask content was poured over ice-cold ether (20 mL). The ether layer was washed with 2 M NaOH solution (15 mL), water (15 mL), and brine solution (15 mL). The ether layer was dried over Na_2SO_4, filtered, and evaporated under reduced pressure. The crude product was purified by flash column chromatography to afford the desired product as a colorless oil (155 mg, 43%). ^{1}H NMR (500 MHz, $CDCl_3$) δ: 7.44 (d, J = 12 Hz, 2H), 6.79 (d, J = 12 Hz, 2H), 5.02 (br s, 1H), 3.96 (t, J = 5 Hz, 2H), 3.50−3.43 (m, 2H), 1.43 (s, 12H).

*2-(4-Chlorophenoxy)ethan-1-amine (**22c**).* To a stirred solution of the *tert*-butyl (2-(4-chlorophenoxy)ethyl)carbamate (155 mg, 0.5 mmol), trifluoroacetic acid (2.5 mL) in DMC (3 mL) was added dropwise over 30 min. The reaction mixture was stirred at 23 °C for 18 h. Then, the solvent was evaporated, and the crude product was dissolved in ethyl acetate (15 mL) and washed with 1 M NaOH aqueous solution (10 mL). The organic layer was dried over anhydrous Na_2SO_4 and evaporated under reduced pressure to afford the desired product as white crystals (80 mg, 82%). ^{1}H NMR (500 MHz, $CDCl_3$) δ: 7.22 (d, J = 9 Hz, 2H), 6.82 (d, J = 9 Hz, 2H), 3.95 (t, J = 5 Hz, 2H), 3.07 (t, J = 5 Hz, 2H), 1.96 (br s, 2H).

General Procedures for the Synthesis of 2-Methyl-*N*-(2-aryloxyethyl)-2-(arylsulfonyl) Propanamide (23−31). A solution of 2-methyl-2-(arylsulfonyl)propanoic acid **7a**, **7c**, **7f** (0.16−0.22 mmol) in dry THF (10 mL) in a 50 mL foil-wrapped rounded-bottom flask (to protect the amine derivatives from light as recommended) was treated with a solution of PyBOP (87 mg, 0.17

https://dx.doi.org/10.1021/acs.jmedchem.0c00371
J. Med. Chem. 2020, 63, 4370−4387

mmol) in THF (1 mL) followed by addition of DIPEA (83 μL). The mixture was stirred at room temperature for 10 min. A solution of the appropriate phenoxyethan-1-amine derivative (0.16 mmol) in THF (1 mL) was added and the reaction mixture was allowed to stir at the same temperature for 1 h. The solvent was removed in vacuo, and the crude product was purified by flash column chromatography using ethyl acetate−hexanes (1:3) as the eluent. The physical characters and the spectral data of the separated products are listed below.

*2-Methyl-N-(2-phenoxyethyl)-2-(phenylsulfonyl) Propanamide (**23**).* Starting with **7a** (50 mg, 0.22 mmol), white crystals (44 mg, 57%). ^{1}H NMR (500 MHz, $CDCl_3$) δ: 7.82 (d, J = 7.5 Hz, 2H), 7.63 (br s, 1H), 7.55 (t, J = 7.5 Hz, 1H), 7.34−7.32 (m, 2H), 7.29−7.27 (m, 2H), 6.97 (t, J = 7.5 Hz, 1H), 6.97 (d, J = 7.5 Hz, 1H), 4.06 (t, J = 5.0 Hz, 2H), 3.70 (q, J = 5.5 Hz, 2H), 1.60 (s, 6H). ^{13}C NMR (500 MHz, $CDCl_3$) δ 168.09, 158.39, 135.09, 134.27, 130.06, 129.69, 129.00, 121.36, 114.56, 67.97, 65.98, 40.01, 20.71. HPLC purity, 100%. ESIMS calcd for $C_{18}H_{21}NO_4S$: 347.12, found mass $[M + H]^+$, 348.08;, $[M + Na]^+$, 370.06. HRMS (m/z): $[M + H]^+$ calcd for $C_{18}H_{21}NO_4S$, 348.1191; found, 348.1263; exact mass (monoisotopic) from spectrum, 347.1190.

*2-Methyl-N-(2-phenoxyethyl)-2-)4-(trifluoromethyl)phenyl-(sulfonyl) Propenamide (**24**).* Starting with **7c** (50 mg, 0.16 mmol), white solid (38 mg, 54%). ^{1}H NMR (500 MHz, $CDCl_3$) δ: 7.94 (d, J = 8.0 Hz, 2H), 7.52 (br s, 1H), 7.46 (d, J = 8.0 Hz, 2H), 7.34 (t, J = 8.0 Hz, 2H), 7.03 (t, J = 7.5 Hz, 1H), 6.97 (d, J = 8.0 Hz, 2H), 4.06 (t, J = 5.0 Hz, 2H), 3.70 (q, J = 5.5 Hz, 2H), 1.64 (s, 6H). ^{13}C NMR (125 MHz, $CDCl_3$) δ 167.64, 158.26, 138.69, 135.91 (q, J = 32.5 Hz), 130.68, 129.81, 126.10 (q, J = 3.75 Hz), 124.47, 67.59, 39.47, 33.09, 20.71.; HPLC purity, 100%. ESIMS calcd for $C_{19}H_{20}F_3NO_4S$: 415.11, found mass $[M + Na]^+$, 438.05.; HRMS (m/z): $[M + H]^+$ calcd for $C_{19}H_{20}F_3NO_4S$, 416.1065; found, 416.1137, exact mass (monoisotopic) from spectrum, 415.1064.

*2-Methyl-N-(2-phenoxyethyl)-2-)5-(trifluoromethyl)pyridin-2-yl-(sulfonyl) Propenamide (**25**).* Starting with **7e** (50 mg, 0.16 mmol), white solid (60 mg, 85%). ^{1}H NMR (500 MHz, $CDCl_3$) δ: 8.79 (s, 1H), 7.93 (d, J = 8.5 Hz, 1H), 7.81 (d, J = 8.5 Hz, 1H), 7.51 (br s, 1H), 7.30−7.27 (m, 2H), 7.00−6.97 (m, 1H), 6.88 (d, J = 8.0 Hz, 2H), 4.01 (t, J = 5.0 Hz, 2H), 3.69 (q, J = 5.5 Hz, 2H), 1.70 (s, 6H). ^{13}C NMR (125 MHz, $CDCl_3$) δ 167.84, 158.46, 158.19, 147.05, 147.02 135.47, 147.02, 130.14 (q, J = 33.75 Hz), 124.35, 121.33, 114.51, 67.83, 66.05, 39.98, 20.55. HPLC purity, 98.5%. ESIMS calcd for $C_{18}H_{19}F_3N_2O_4S$: 416.10, found mass $[M + H]^+$, 417.10; $[M + Na]^+$, 439.04. HRMS (m/z): $[M + H]^+$ calcd for $C_{18}H_{19}F_3N_2O_4S$, 417.1018; found, 417.1090; exact mass (monoisotopic) from spectrum, 416.1018.

*N-(2-(2-Chlorophenoxy)ethyl)-2-methyl-2-(Phenylsulfonyl) Propanamide (**26**).* Starting with **7a** (50 mg, 0.22 mmol), white solid (40 mg, 48%). ^{1}H NMR (500 MHz, $CDCl_3$) δ: 7.85 (d, J = 7.5 Hz, 2H), 7.60 (br s, 1H), 7.57 (t, J = 7.5 Hz, 2H), 7.40 (d, J = 7.5 Hz, 1H), 7.35 (m, 2H), 7.24 (m, 1H), 6.97−6.93 (m, 2H), 4.12 (t, J = 5.0 Hz, 2H), 3.74 (q, J = 5.0 Hz, 2H), 1.60 (s, 6H). ^{13}C NMR (500 MHz, $CDCl_3$) δ 168.13, 153.95, 135.15, 134.26, 130.53, 130.14, 128.93, 127.85, 123.26, 122.14, 113.69, 68.02, 67.34, 39.88, 20.72. HPLC purity, 100%. ESIMS calcd for $C_{18}H_{20}ClNO_4S$: 381.08, found mass $[M + H]^+$, 382.05; $[M + Na]^+$, 404.03. HRMS (m/z): $[M + H]^+$ calcd for $C_{18}H_{20}ClNO_4S$, 382.0802; exact mass (monoisotopic) from spectrum, 381.0800.

*N-(2-(2-Chlorophenoxy)ethyl)-2-methyl-2-((4-(trifluoromethyl)-phenyl)sulfonyl) Propanamide (**27**).* Starting with **7c** (50 mg, 0.16 mmol), white solid (53 mg, 70%). ^{1}H NMR (500 MHz, $CDCl_3$) δ: 7.98 (d, J = 8.5 Hz, 1H), 7.55 (d, J = 8.5 Hz, 1H), 7.52 (br s, 1H), 7.42−7.40 (m, 1H), 7.27−7.23 (m, 1H), 6.99−6.96 (m, 1H), 6.94−6.92 (m, 1H), 4.12 (t, J = 5.0 Hz, 2H), 3.73 (q, J = 5.0 Hz, 2H), 1.62 (s, 6H). ^{13}C NMR (500 MHz, $CDCl_3$) δ 167.69, 153.82, 138.81, 135.90 (q, J = 32.5 Hz), 130.77, 130.59, 127.95, 125.97, 124.05, 123.17, 122.31, 113.66, 68.31, 67.24, 40.03, 20.52. HPLC purity, 97.4%. ESIMS calcd for $C_{19}H_{19}ClF_3NO_4S$: 449.07, found mass $[M + H]^+$, 450.01; $[M + Na]^+$, 472.00. HRMS (m/z): $[M + H]^+$ calcd for $C_{19}H_{19}ClF_3NO_4S$, 450.0675; found, 450.0751; exact mass (monoisotopic) from spectrum, 449.0678.

*N-(2-(2-Chlorophenoxy)ethyl)-2-methyl-2-((5-(trifluoromethyl)-pyridin-2-yl)sulfonyl) Propanamide (**28**).* Starting with **7e** (50 mg, 0.16 mmol), white solid (64 mg, 84%). ^{1}H NMR (500 MHz, $CDCl_3$) δ: 8.75 (s, 1H), 8.11 (d, J = 8.5 Hz, 1H), 7.81 (d, J = 8.5 Hz, 1H), 7.51 (br s, 1H), 7.38−7.36 (m, 2H), 7.22 (t, J = 7.5 Hz, 1H), 6.96−6.92 (m, 1H), 6.81 (d, J = 8.0 Hz, 1H), 4.09 (t, J = 5.0 Hz, 2H), 3.73 (q, J = 5.5 Hz, 2H), 1.70 (s, 6H). ^{13}C NMR (DMSO-d_6) δ 167.94, 158.44, 153.93, 146.97, 146.94, 135.41, 130.49, 129.91, 127.87, 124.40, 123.16, 122.17, 113.70, 67.95, 67.35, 39.86, 20.56. HPLC purity, 97.8%. ESIMS calcd for $C_{18}H_{18}ClF_3N_2O_4S$: 450.06, found mass $[M + H]^+$, 451.05. HRMS (m/z): $[M + H]^+$ calcd for $C_{18}H_{18}ClF_3N_2O_4S$, 451.0704; found, 450.0751; exact mass (monoisotopic) from spectrum, 450.0631.

*N-(2-(4-Chlorophenoxy)ethyl)-2-methyl-2-(phenylsulfonyl) Propanamide (**29**).* Starting with **7a** (50 mg, 0.22 mmol), white solid (21 mg, 25%). ^{1}H NMR (500 MHz, $CDCl_3$) δ: 8.12 (d, J = 7.5 Hz, 2H), 7.58 (t, J = 7.5 Hz, 2H), 7.33 (d, J = 7.5 Hz, 2H), 7.28−7.26 (m, 2H), 6.88 (d, J = 10.5 Hz, 2H), 4.03 (t, J = 5.0 Hz, 2H), 3.68 (q, J = 5.0 Hz, 2H), 1.58 (s, 6H). ^{13}C NMR (125 MHz, $CDCl_3$) δ 168.11, 157.01, 135.05, 134.36, 130.03, 129.57, 129.02, 126.30, 115.85, 67.97, 66.44, 39.87, 20.77. HPLC purity, 99.5%. ESIMS calcd for $C_{18}H_{20}ClNO_4S$: 381.08, found mass $[M + H]^+$, 382.20. HRMS (m/z): $[M + H]^+$ calcd for $C_{18}H_{20}ClNO_4S$, 382.0802; found, 382.0873; exact mass (monoisotopic) from spectrum, 381.0800.

*N-(2-(4-Chlorophenoxy)ethyl)-2-methyl-2-((4-(trifluoromethyl)-phenyl)sulfonyl) Propanamide (**30**).* Starting with **7c** (50 mg, 0.16 mmol), white solid (54 mg, 71%). ^{1}H NMR (500 MHz, $CDCl_3$) δ: 7.94 (d, J = 8.0 Hz, 2H), 7.56 (d, J = 8.5 Hz, 2H), 7.45 (br s, 1H), 7.29−7.26 (m, 2H), 6.90−6.87 (m, 2H), 4.03 (t, J = 5.0 Hz, 2H), 3.68 (q, J = 5.5 Hz, 2H), 1.60 (s, 6H). ^{13}C NMR (125 MHz, $CDCl_3$) δ 167.60, 156.90, 138.69, 135.65 (q, J = 32.5 Hz), 130.67, 129.64, 126.52, 126.11, 124.01, 115.84, 68.27, 66.37, 39.99, 20.58. ^{19}F NMR δ −63.41 (s). HPLC purity, 98.7%. ESIMS calcd for $C_{19}H_{19}ClF_3NO_4S$: 449.07; found mass $[M + H]^+$, 450.03. HRMS (m/z): $[M + H]^+$ calcd for $C_{19}H_{19}ClF_3NO_4S$, 450.0675; found, 450.0750; exact mass (monoisotopic) from spectrum, 449.0677.

*N-(2-(4-Chlorophenoxy)ethyl)-2-methyl-2-((5-(trifluoromethyl)-pyridin-2-yl)sulfonyl) Propenamide (**31**).* Starting with **7e** (50 mg, 0.16 mmol), white solid (43 mg, 57%). ^{1}H NMR (500 MHz, $CDCl_3$) δ: 8.76 (s, 1H), 8.13 (d, J = 8.5 Hz, 1H), 7.98 (d, J = 8.0 Hz, 1H), 7.49 (br s, 1H), 7.22 (d, J = 8.5 Hz, 2H), 6.82 (d, J = 8.5 Hz, 2H), 4.02 (t, J = 5.0 Hz, 2H), 3.68 (q, J = 5.0 Hz, 2H), 1.66 (s, 6H). ^{13}C NMR (125 MHz, $CDCl_3$) δ 167.90, 158.22, 157.11, 147.04, 135.47, 129.87 (q, J = 33.75 Hz), 129.46, 126.25, 124.25, 123.38 115.85, 67.64, 66.51, 39.84, 20.54. HPLC purity, 97.8%. ESIMS calcd for $C_{18}H_{18}ClF_3N_2O_4S$: 450.06; found mass $[M + H]^+$, 451.01; $[M + Na]^+$, 473.01. HRMS (m/z): $[M + H]^+$ calcd for $C_{18}H_{18}ClF_3N_2O_4S$, 451.0628; found, 451.0703; exact mass (monoisotopic) from spectrum, 450.0630.

General Procedure for Synthesis of 1-(4-Arylpiperazin-1-yl)-2-((5-(trifluoromethyl)pyridin-2-yl)sulfonyl)alkyl-1-one (33−45). To a stirred solution of the appropriate carboxylic acid derivative (**7d** and **7e** 50 mg, 0.16−0.17 mmol) in dry THF (10 mL), a solution of PyBOP (87 mg, 0.17 mmol) in THF (1 mL) followed by DIPEA (83 μL) were added. Then, the mixture was stirred at room temperature for 10 min under nitrogen gas before a solution of the appropriate 4-aryl piperazine (0.16−0.17 mmol) in THF (1 mL) was added. The resulting yellow solution was allowed to stir at room temperature for 1 h. The solvent was removed under reduced pressure, and the crude product was absorbed onto silica gel and purified by flash column chromatography using ethyl acetate/hexane as the eluent to afford the desired product as the following.

*2-Methyl-1-(4-phenylpiperazin-1-yl)-2-((5-(trifluoromethyl)-pyridin-2-yl)sulfonyl) Propan-1-one (**33**).* Starting with **7e** (50 mg, 0.16 mmol) and 1-phenylpiperazine (25 μL, 0.16 mmol), off-white solid (42 mg, 61%). ^{1}H NMR (500 MHz, $CDCl_3$) δ: 8.94 (s, 1 H), 8.23 (d, J = 8.5 Hz, 1H), 8.19 (d, J = 12.0 Hz, 1H), 7.29 (d, J = 7.5 Hz, 2H), 6.95−6.92 (m, 3H), 3.91 (s, 4H), 3.26 (s, 4H), 1.87 (s, 6H). ^{13}C NMR (125 MHz, $CDCl_3$) δ 166.62, 160.05, 146.83, 135.41, 135.40, 129.98, 129.71, 124.57, 123.75, 121.57, 120.68, 116.61, 71.54,

https://dx.doi.org/10.1021/acs.jmedchem.0c00371
J. Med. Chem. 2020, 63, 4370−4387

49.48, 45.75, 22.90. HPLC purity, 97.49%. ESIMS calcd for $C_{20}H_{22}F_3N_2O_3S$: 441.13; found mass $[M + H]^+$, 442.50. HRMS (m/z): $[M + H]^+$ calcd for $C_{20}H_{22}F_3N_2O_3S$, 442.1334; found, 442.1404; exact mass (monoisotopic) from spectrum, 441.1331.

*2-Methyl-1-(4-(pyridin-2-yl)piperazin-1-yl)-2-((5-(trifluoromethyl)pyridin-2-yl)sulfonyl) Propan-1-one (**34**).* Starting with **7e** (50 mg, 0.16 mmol) and 1-(pyridin-2-yl)piperazine (28 μL, 0.16 mmol), off-white solid (57 mg, 81%). ^{1}H NMR (500 MHz, $CDCl_3$) δ: 8.94 (s, 1 H), 8.24−8.17 (m, 3H), 7.53 (d, J = 7.0 Hz, 1H), 6.70−6.66 (m, 2H), 3.88 (s, 4H), 3.66−3.65 (m, 4H), 1.87 (s, 6H). ^{13}C NMR (125 MHz, $CDCl_3$) δ 166.62, 159.93, 158.76, 147.62, 146.70, 137.98, 135.30, 129.71 (q, J = 33.75 Hz), 124.45, 123.64, 114.00, 107.45, 71.44, 45.19, 22.73. HPLC purity, 97.69%. ESIMS calcd for $C_{19}H_{21}F_3N_4O_3S$: 442.13; found mass $[M + H]^+$, 443.39. HRMS (m/z): $[M + H]^+$ calcd for $C_{19}H_{21}F_3N_4O_3S$, 443.1286; found, 443.1357; exact mass (monoisotopic) from spectrum, 442.1284.

*2-Methyl-1-(4-(o-tolyl)piperazin-1-yl)-2-((5-(trifluoromethyl)-pyridin-2-yl)sulfonyl) Propan-1-one (**35**).* Starting with **7e** (50 mg, 0.16 mmol) and 1-(*o*-tolyl)piperazine (30 μL, 0.16 mmol), white solid (40 mg, 56%). ^{1}H NMR (500 MHz, $CDCl_3$) δ: 8.95 (s, 1 H), 8.26 (d, J = 8.0 Hz, 1H), 8.19 (d, J = 7.5 Hz, 1H), 7.20−7.15 (m, 2H), 7.03−6.99 (m, 2H), 3.87 (s, 4H), 2.95 (s, 3H), 2.32 (s, 3H), 1.90 (s, 6H). ^{13}C NMR (125 MHz, $CDCl_3$) δ 166.75, 160.47, 150.60, 146.66, 135.26, 132.71, 131.25, 129.75, 129.48, 126.73, 124.40, 123.88, 119.16, 71.84, 51.77, 22.76, 17.83. HPLC purity, 97.9%. ESIMS calcd for $C_{21}H_{24}F_3N_2O_3S$: 455.16; found mass $[M + H]^+$, 456.53. HRMS (m/z): $[M + H]^+$ calcd for $C_{21}H_{24}F_3N_2O_3S$, 456.1490; found, 456.1561; exact mass (monoisotopic) from spectrum, 455.1489.

*1-(4-(2,5-Dimethylphenyl)piperazin-1-yl)-2-methyl-2-((5-(trifluoromethyl)pyridin-2-yl)sulfonyl) Propan-1-one (**36**).* Starting with **7e** (50 mg, 0.16 mmol) and 1-(2,5-dimethylphenyl) piperazine (32 μL, 0.16 mmol), white solid (65 mg, 88%). ^{1}H NMR (500 MHz, $CDCl_3$) δ: 8.96 (s, 1 H), 8.26 (d, J = 8.5 Hz, 1H), 8.20 (d, J = 8.0 Hz, 1H), 7.08 (d, J = 7.5 Hz, 1H), 6.82 (m, 2H), 3.86 (s, 4H), 2.95 (s, 4H), 2.30 (s, 3H), 2.27 (s, 3H), 1.90 (s, 6H). ^{13}C NMR (125 MHz, $CDCl_3$) δ 166.73, 160.51, 150.43, 146.64, 136.33, 135.26, 131.05, 129.39, 124.49, 124.39, 123.70, 119.92, 71.87, 51.78, 22.76, 21.15, 17.41. HPLC purity, 98.9%. ESIMS calcd for $C_{22}H_{26}F_3N_3O_3S$: 469.16; found mass $[M + H]^+$, 470.24. HRMS (m/z): $[M + H]^+$ calcd for $C_{22}H_{26}F_3N_3O_3S$, 470.1647; found, 470.1719; exact mass (monoisotopic) from spectrum, 469.1647.

*1-(4-(3,4-Dichlorophenyl)piperazin-1-yl)-2-((5-(trifluoromethyl)-pyridin-2-yl)sulfonyl) Propan-1-one (**37**).* Starting with **7e** (50 mg, 0.16 mmol) and 1-(3,4-dichlorophenyl) piperazine (39 mg, 0.16 mmol), white crystals (53 mg, 61.5%). ^{1}H NMR (500 MHz, $CDCl_3$) δ: 8.91 (s, 4 H), 8.21−8.19 (m, 2H), 7.30−7.28 (m, J = 9.0 Hz,1H), 6.96 (s, 1H), 6.76−6.73 (m, 1H), 3.99 (m, 4H), 3.25−3.23 (m, 4H), 1.83 (s, 6H). ^{13}C NMR (125 MHz, $CDCl_3$) δ 166.38, 159.48, 150.12, 146.82, 135.34, 133.00, 130.63, 130.03, 129.76, 124.49, 123.10, 117.64, 115.65, 71.04, 48.78, 45.50, 22.90. HPLC purity, 98.1%. ESIMS calcd for $C_{20}H_{20}Cl_2F_3N_3O_3S$: 509.06; found mass $[M + H]^+$, 510.16. HRMS (m/z): $[M + H]^+$ calcd for $C_{20}H_{20}Cl_2F_3N_3O_3S$, 510.0555; found, 510.0636; exact mass (monoisotopic) from spectrum, 509.0564.

*1-(4-(3-Methoxyphenyl)piperazin-1-yl)-2-methyl-2-((5-(trifluoromethyl)pyridin-2-yl)sulfonyl) Propan-1-one (**38**).* Starting with **7e** (50 mg, 0.16 mmol) and 1-(*m*-methoxyphenyl) piperazine (30 μL, 0.16 mmol), white solid (80 mg, 97.5%). ^{1}H NMR (500 MHz, $CDCl_3$) δ: 8.93 (s, 1 H), 8.22 (d, J = 8.0 Hz, 1H), 8.17 (d, J = 8.5 Hz, 1H), 7.18 (t, J = 8.5 Hz, 1H), 6.54−6.52 (m, 1H), 6.46−6.45 (m, 2H), 3.88 (s, 4H), 3.78 (s, 3H), 3.25−3.24 (s, 4H), 1.86 (s, 6H). ^{19}F NMR δ −62.62 (s). ^{13}C NMR (125 MHz, $CDCl_3$) δ 166.51, 160.69, 159.94, 152.09, 146.73, 146.70 135.28, 135.25, 129.99, 124.44, 109.06, 105.22, 102.90, 71.42, 55.24, 49.20, 22.79. HPLC purity, 97.5%. ESIMS calcd for $C_{21}H_{24}F_3N_3O_4S$: 471.14; found mass $[M + H]^+$, 472.14. HRMS (m/z): $[M + H]^+$ calcd for $C_{21}H_{24}F_3N_3O_4S$, 472.1439; found, 472.1511; exact mass (monoisotopic) from spectrum, 471.1439.

*2-Methyl-1-(4-(4-fluorobenzyl)piperazin-1-yl]2-((5-(trifluoromethyl)pyridin-2-yl)sulfonyl) Propan-1-one (**39**).* Starting with **7e** (50 mg, 0.16 mmol) and 1-(4-fluorobenzyl)piperazine (33 mg, 0.16 mmol), white solid (42 mg, 53%). ^{1}H NMR (500 MHz, $CDCl_3$) δ: 8.91 (s, 1 H), 8.22 (d, J = 8.5 Hz, 1H), 8.17 (d, J = 8.0 Hz, 1H), 7.28−7.25 (m, 2H), 7.27 (t, J = 8.5 Hz, 2H), 3.70 (s, 4H), 3.48 (s, 2H), 2.47 (s, 4H), 1.87 (s, 6H). ^{13}C NMR (125 MHz, $CDCl_3$) δ 166.54, 161.18, 160.49, 146.58, 135.24, 133.12, 130.66, 130.59, 124.37, 115.29, 115.12, 71.83, 61.92, 52.74, 22.63. ^{19}F NMR δ −62.61, −70.08, −71.60. HPLC purity, 97.9%. ESIMS calcd for $C_{21}H_{23}F_4N_2O_3S$: 473.14; found mass $[M + H]^+$, 474.30. HRMS (m/z): $[M + H]^+$ calcd for $C_{21}H_{23}F_4N_2O_3S$, 474.1396; found, 474.1467; exact mass (monoisotopic) from spectrum, 4731394.

*2-Methyl-1-(4-(4-Chlorobenzyl)piperazin-1-yl)-2-((5-(trifluoromethyl)pyridin-2-yl)sulfonyl) Propan-1-one (**40**).* Starting with **7e** (50 mg, 0.16 mmol) and 1-(4-chlorobenzyl)piperazine (30 μL, 0.16 mmol), white solid (69 mg, 84.1%). ^{1}H NMR (500 MHz, $CDCl_3$) δ: 8.91 (s, 1 H), 8.22 (d, J = 8.0 Hz, 1H), 8.18 (d, J = 8.0 Hz, 1H), 7.31−7.28 (m, 4H), 3.73 (s, 4H), 3.52 (s, 2H), 2.51 (s, 3H), 2.170 (s, 2H), 1.83 (s, 6H). ^{13}C NMR (125 MHz, $CDCl_3$) δ 166.54, 160.51, 146.57, 136.10, 135.26, 133.03, 130.36, 129.52 (q, J = 33.75 Hz), 128.51, 124.37, 123.69, 121.51, 71.84, 61.94, 52.78, 45.62, 22.61. HPLC purity, 99.3%. ESIMS calcd for $C_{21}H_{23}ClF_3N_3O_3S$: 489.11; found mass $[M + H]^+$, 490.14. HRMS (m/z): $[M + H]^+$ calcd for $C_{21}H_{23}ClF_3N_3O_3S$, 490.1101; found, 490.1175; exact mass (monoisotopic) from spectrum, 489.1102.

*2-Methyl-1-(4-(3-chlorobenzyl)piperazin-1-yl)-2-((5-(trifluoromethyl)pyridin-2-yl)sulfonyl) Propan-1-one (**41**).* Starting with **7e** (50 mg, 0.16 mmol) and 1-(3-chlorobenzyl)piperazine (30 μL, 0.16 mmol), white solid (72 mg, 88%). ^{1}H NMR (500 MHz, $CDCl_3$) δ: 8.91 (s, 1 H), 8.22 (d, J = 8.0 Hz, 1H), 8.17 (d, J = 8.0 Hz, 1H), 7.32 (s, 1H), 7.24−7.17 (m, 3H), 3.72−3.67 (m, 4H), 3.49 (s, 2H), 2.49−2.47 (m, 4H), 1.84 (s, 6H). ^{13}C NMR (125 MHz, $CDCl_3$) δ 166.56, 160.50, 146.59, 144.60, 139.87, 135.21, 134.34, 129.63, 129.00, 127.54, 127.13, 124.36, 71.81, 62.11, 55.91, 52.83, 22.65. HPLC purity, 98.87%. ESIMS calcd for $C_{21}H_{23}ClF_3N_3O_3S$: 489.11; found mass $[M + H]^+$, 490.17. HRMS (m/z): $[M + H]^+$ calcd for $C_{21}H_{23}ClF_3N_3O_3S$, 490.1101; found, 490.1173; exact mass (monoisotopic) from spectrum, 489.1100.

*2-Methyl-1-(4-(4-methylbenzyl)piperazin-1-yl)-2-((5-(trifluoromethyl)pyridin-2-yl)sulfonyl) Propan-1-one (**42**).* Starting with **7e** (50 mg, 0.16 mmol) and 1-(4-methylbenzyl)piperazine (32 mg, 0.16 mmol), white solid (40 mg, 51%). ^{1}H NMR (500 MHz, $CDCl_3$) δ: 8.86 (s, 1 H), 8.22 (d, J = 8.5 Hz, 1H), 8.17 (d, J = 8.0 Hz, 1H), 7.22 (d, J = 7.5 Hz, 1H), 7.14 (d, J = 7.5 Hz, 1H), 3.73 (s, 4H), 3.55 (s, 2H), 2.53 (s, 4H), 2.34 (s, 3H), 1.84 (s, 6H). ^{13}C NMR (125 MHz, $CDCl_3$) δ 166.59, 160.64, 146.53, 137.04, 135.22, 134.17, 129.18, 129.05, 124.37, 123.70, 121.53, 71.98, 62.47, 52.71, 45.70, 22.55, 21.11. HPLC purity, 95.9%. ESIMS calcd for $C_{22}H_{26}F_3N_3O_3S$: 469.16; found mass $[M + H]^+$, 470.58. HRMS (m/z): $[M + H]^+$ calcd for $C_{22}H_{26}F_3N_3O_3S$, 470.1647; found, 470.1722; exact mass (monoisotopic) from spectrum, 469.1649.

*1-(4-(o-Tolyl)piperazin-1-yl)-2-((5-(trifluoromethyl)pyridin-2-yl)-sulfonyl)propan-1-one (**43**).* Starting with **7d** (50 mg, 0.17 mmol) and 1-(*o*-tolyl)piperazine (33 μL, 0.17 mmol), yellowish-white solid (52 mg, 67%). ^{1}H NMR (500 MHz, $CDCl_3$) δ: 9.01 (s, 1 H), 8.24 (s, 2H), 7.19 (m, 2H), 7.01 (d, J = 7.5 Hz, 2H), 4.97 (q, J = 7.0 Hz, 1H), 3.96−3.71 (m, 4H), 3.15−2.93 (m, 4H), 2.36 (s, 3H), 1.62 (d, J = 7.0 Hz, 3H). ^{13}C NMR (125 MHz, $CDCl_3$) δ 163.32, 159.20, 150.53, 147.01, 135.72, 132.72, 131.24, 130.10 (q, J = 33.75 Hz), 126.75, 123.94, 123.61, 121.43, 119.27, 58.80, 51.94, 51.53, 47.33, 43.23, 17.81, 13.37. HPLC purity, 98.3%. ESIMS calcd for $C_{19}H_{22}F_3N_3O_3S$: 441.13; found mass $[M + H]^+$, 442.01. HRMS (m/z): $[M + H]^+$ calcd for $C_{19}H_{22}F_3N_3O_3S$, 442.1334; found, 442.1406; exact mass (monoisotopic) from spectrum, 441.1334.

*1-(4-(2,5-Dimethylphenyl)piperazin-1-yl)-2-((5-(trifluoromethyl)-pyridin-2-yl)sulfonyl) Propan-1-one (**44**).* Starting with **7d** (50 mg, 0.17 mmol) and 1-(2,5-dimethylphenyl)piperazine (35 μL, 0.17 mmol), white solid (51 mg, 64%). ^{1}H NMR (500 MHz, $CDCl_3$) δ: 9.01 (s, 1 H), 8.23 (s, 2H), 7.19 (d, J = 7.5 Hz, 1H), 7.06−7.03 (m, 2H), 4.97 (q, J = 7.0 Hz, 1H), 3.96−3.68 (m, 4H), 3.13−2.90 (m, 4H), 2.30 (s, 6H), 1.62 (d, J = 7.0 Hz, 3H). ^{13}C NMR (125 MHz,

https://dx.doi.org/10.1021/acs.jmedchem.0c00371
J. Med. Chem. 2020, 63, 4370−4387

$CDCl_3$) δ 163.28, 159.20, 150.38, 147.02, 136.36, 135.67, 131.04, 130.25, 129.98, 129.41, 124.59, 123.94, 120.04, 58.83, 51.93, 51.56, 47.36, 43.26, 21.13, 17.38, 13.36. HPLC purity, 99.7%. ESIMS calcd for $C_{21}H_{24}F_3N_3O_3S$: 455.15; found mass $[M + H]^+$, 456.17. HRMS (m/z): $[M + H]^+$ calcd for $C_{21}H_{24}F_3N_3O_3S$, 456.1490; found, 456.1560; exact mass (monoisotopic) from spectrum, 455.1487.

*1-(4-(3,4-Dichlorophenyl)piperazin-1-yl)-2-((5-(trifluoromethyl)-pyridin-2-yl)sulfonyl) Propan-1-one (**45**).* Starting with **7d** (50 mg, 0.17 mmol) and 1-(3,4-dichlorophenyl)piperazine (40 mg, 0.17 mmol), shiny white crystals (31 mg, 58%). ^1H NMR (500 MHz, $CDCl_3$) δ: 9.00 (s, 1 H), 8.42−8.20 (m, 2H), 7.30 (d, J = 9.0 Hz, 1H), 6.97 (s, 1H), 6.75 (dd, J = 6.0 Hz, 1H), 4.97 (q, J = 7.0 Hz, 1H), 4.03−3.11 (m, 8H), 1.58 (d, J = 8.0 Hz, 3H). ^{13}C NMR (125 MHz, $CDCl_3$) δ 162.96, 158.88, 150.05, 147.12, 135.78, 133.00, 130.66, 123.86, 123.54, 123.31, 121.36, 117.94, 115.92, 58.44, 49.06, 48.78, 46.33, 42.37, 13.38. HPLC purity (methanol−water, 1:1), 95.4%. ESIMS $[M + H]^+$ calcd for $C_{19}H_{18}C_{l2}F_3N_3O_3S$: 497.04; found mass $[M + H]^+$, 497.15. HRMS (m/z): $[M + H]$ calcd for $C_{21}H_{24}F_3N_3O_3S$, 496.0398; found, 496.0474; exact mass (monoisotopic) from spectrum, 495.0401.

Biology. *Cell Culture, Chlamydia trachomatis Propagation, and IFU Assay.* The human epithelial cell line HEp-2 was routinely propagated in Dulbecco's modified Eagle medium (DMEM; Gibco) supplemented with 2% L-glutamine and 10% fetal bovine serum (FBS) at 37 °C with 5% CO_2. All infected and uninfected cell cultures were incubated at these conditions. Compounds stocks of the synthesized compounds were prepared in sterile dimethyl sulfoxide (50 mg/mL) and frozen at −20 °C in 5 μL aliquots.[41]

To quantify the effect of the most active compounds on *C. trachomatis*, HEp-2 cells were first seeded in a 24-well plate. Cells were infected with *C. trachomatis* L2 at a multiplicity of infection of 1, and the tested compounds were added in triplicate 8 h postinfection (hpi). At 24 hpi, cell lysates, which contain *C. trachomatis* elementary bodies, were collected from infected HEp-2 cell cultures in sucrose storage medium. The resulting mixture was frozen at −80 °C and used to infect a fresh HEp2 cell monolayer in a series of 10-fold dilutions. After a further 24 hpi, the recoverable EBs from the initial infection were stained using primary goat anti-MOMP antibody and a secondary donkey antigoat antibody labeled with Alexa488. The fluorescent inclusions were counted from 15 fields of view (FOV) at 20× magnification. IFUs were calculated as the average count of inclusions in each FOV corrected for the dilution factor.[41,87] In the mechanism of action assays, we followed the same protocol described in the IFU assay. For (24 h reactivation) samples, the DMEM medium was removed after 24 hpi and the wells were washed three times with Hanks' balanced salt solution and fresh medium without compounds was added (0.5 mL/well).

Casein Degradation Assay. All recombinant, C-terminal 6X His-tagged ClpP proteins were expressed using *E. coli* and purified as previously described using a *clpAPX*-null *E. coli* strain kindly provided by Dr. Peter Sass.[41,42] The *clpP* human (NM_006012.4) and mouse (NM_017393.2) mRNA sequences were used to obtain the ClpP-encoding ORF minus the mitochondrial localization signal. Genes were then codon optimized for *E. coli* expression and synthesized by Integrated DNA Technologies. The mouse and human *clpP* paralogues were cloned into the pLATE31 vector (Thermo Scientific) as previously performed for the bacterial ClpPs. Examples of purified protein samples are shown in Figure S2. FITC-casein (Sigma-Aldrich, C0528) was treated with Zeba 7K cutoff spin columns (Thermo Scientific) to remove free FITC. Assays were carried out in buffer PZ (25 mM HEPES [pH 7.6], 200 mM KCl, 5 mM $MgCl_2$, 1 mM DTT, and 10% v/v of glycerol) using 100 μL reactions and 20 μM FITC-casein. 1 μM or 0.1 μM (for **40**) of ClpP from *E. coli*, 1 μM mouse or human ClpP, or 6 μM of ClpP1 and ClpP2 were preincubated with either 25 μg/μL compounds or DMSO solvent at 32 °C for 30 min before adding FITC-casein. Reactions were monitored for 3 h with readings every 3 min on a Tecan m Plex plate reader using an excitation wavelength of λex = 490 nm and an emission wavelength λem = 525 nm. Reactions were run at least three times using at least two independent protein purification preparations.

Antibacterial Assay against Additional Strains. *S. aureus* USA 300 JE2 and *E. coli* K12 were provided by the Dr. Bayles' research lab at the Department of Pathology and Microbiology of the University of Nebraska Medical Center (UNMC). The MICs of the synthesized compounds were tested in triplicate samples, using the broth microdilution method as previously reported.[88] The bacterial cultures were made in Muller Hinton Broth (MHB) using the direct colony suspension method at 1.5×10^8 CFU/mL, followed by dilution to $\sim 10^5$ CFU/mL. The stock solutions of the tested compounds were prepared in sterile DMSO at 1 mg/mL concentration. Then, serial dilutions of the tested compounds were made in MHB in Cellstar 96-well microtiter plates using vancomycin as a positive control, and blank media as a negative control. 10 μL of bacterial culture was added per well followed by incubating the plates for 16 h at the optimum temperature. The MIC was categorized as the concentration at which no visible growth of bacteria was observed at 600 nm in a particular well using an AccuSkan, MultiSkan FC. The average of triplicate MIC determinations is reported (for further details please see the Supporting Information).

Cytotoxicity Assay (CCK-8). The immortal keratinocyte cell line (HaCaT) and HeLa 229 were cultured in DMEM media containing 10% FBS and 1% penicillin/streptomycin solution at 37 °C with 5% CO_2. The cells were seeded separately at a density of 5000 cells per well in 96-well plates. On the next day, cells were treated with 50 μg/mL of the tested drugs in triplicate, and as controls we used DMSO at a concentration equivalent to the one used in drug-treated cells. Then, the plates were incubated for an additional 24 h before the addition of 10 μL of the assay reagent Cell Counting Kit-8 (CCK-8) (DOJINDO laboratories) followed by incubation of the plates for 2 h. Corrected absorbance readings were determined with a 450 nm filter using a multiscan FC microplate photometer (Thermo Fisher Scientific).

Mutagenic Studies: SMART. We assessed the mutagenicity of the compounds by Somatic Mutation and Recombination Test (SMART) using wing-somatic cells of *Drosophila melanogaster*.[89,90] The following 3 crosses of mutant flies were set up: (1) Standard cross (ST): *flare-3* (flr^3) virgin females, with genetic constituent $flr^3/In(3LR)TM3$, *ri* $p^p se^p I(3)89Aa$ $bx^{34e}e$ Bd^S crossed with *multiple wing hairs* (*mwh*) males, with genetic constituent *y*; *mwh jv* and (2) High bioactivation (HB) cross: *ORR*; *flare* (*ORR*; *flr3*) virgin female, with genetic constituent *ORR*; flr^3/In (*3LR*) *TM3, ri pp sep I(3)89 Aa bx 34e* Bd^S crossed with *mwh* males. The *ORR;flr3* strain carries the chromosomes 1 and 2 from a DDT-resistant Oregon R (R) line, which contain genes responsible for the high level of metabolizing enzymes of the cytochrome P450, P(CYP)6 A2 type.[89]

Eggs were collected from flies of the two different crosses in culture flasks containing a solid agar−agar base (5% w/v), covered by a layer of live baker's yeast supplemented with sugar for 8 h. Third instar larvae (72 ± 4 h) were washed out of the culture bottles with tap water and collected with a fine meshed strainer. Larvae groups were transferred to glass vials containing hydrated alternative medium (instant mashed potato flakes Yoki) and exposed to compounds **11**, **20**, **24**, **26**, **40**, and **41** at 0.25, 0.5, and 1.0 mM final concentrations. Solvent (Milli-Q water, 1% of Tween-80, and 3% ethanol) was used as a negative control.

The hatched flies of the marker heterozygote (*mwh* + /+ *flr3*) and the balancer heterozygote (*mwh* + /+ *TM3, Bds*) genotypes were collected and fixed in 70% ethanol. Wings were removed, mounted on slides containing Faure's solution (30 g of gum Arabic, 50 g of chloral hydrate, 20 mL of glycerol, and 50 mL of water), and analyzed under anoptical microscope (400×) for the occurrence of different types of mutant spots.[91]

The statistical analysis was performed as described by Frei and Würgler,[90] using the chi-squared test. Results were considered statistically significant when $p < 0.05$. The frequencies of each spot (single small, single large, or twin) and the total frequency of spots per fly, for each treatment, were compared in pairs (i.e., negative control versus compound-treated).

Metabolic Stability. The *in vitro* metabolism stability experiment was done using human liver microsomes (XenoTech, LLC, Lenexa, KS) for phase I metabolism. The results were expressed as the

https://dx.doi.org/10.1021/acs.jmedchem.0c00371
J. Med. Chem. 2020, 63, 4370−4387

percentage of drug remaining (solution were 1 μM in 0.1% methanol), and the studies were performed in triplicate as described previously.[92] For the microsomal stability test, we used a solution of phosphate buffer (100 mM, pH 7.4), microsomal protein (1.0 mg/mL), magnesium chloride (10 mM), and NADPH (2 mM) at a final volume of 1.0 mL. This mixture was preincubated at 37 °C for 10 min in a water bath maintained at 60 rpm. The reaction was initialized by adding the selected compounds (1 μg/mL). Aliquots (100 μL) were collected at 0, 5, 15, 20, 30, 45, and 60 min. The reaction was quenched by adding MeOH (300 μL) containing IS (100 ng/mL). The aliquot and quenching reaction were contained in a 1.5 mL Eppendorf tube. The incubation without the addition of NADPH was used as a negative control. Testosterone was incubated similarly as positive control substrates. Then, 5 μL samples of the supernatants were analyzed by LC−MS/MS.

LC−MS/MS Assay. (A) A Shimadzu LC−MS/MS system (LC−MS/MS 8060, Shimadzu, Japan) was utilized for analysis. The LC system consisted of two LC-30 AD pumps and a CTO-30AS column oven plus an autosampler (SIL-30AC), which was used to inject 10 μL aliquots of the processed samples. The MS/MS system operated at unit resolution in the multiple reaction monitoring (MRM) mode. The following precursor ion > product ion combinations were used: 489.95 > 280.15, 510.05 > 280.05, 417.10 > 280.10, 416.15 > 98.10, and 414.10 > 176.25 *m/z* for **40**, **37**, **25**, **24**, and **11**, respectively. The compound dependent mass spectrometer parameters, such as temperature, voltage, gas pressure, etc., were optimized by auto method optimization via precursor ion search for each analyte and the internal standard (IS) using a 0.5 μg/mL solution in methanol.

(B) Chromatographic separation was achieved on an ACE Excel C_{18} column (1.7 μm, 100 mm × 2.1 mm, from Advance Chromatography Technologies Ltd., U.K.) with a Phenomenex C_{18} guard column (Phenomenex, Torrance, CA). The mobile phase consisted of formic acid in water (0.1%, solvent A) and methanol (MeOH) (solvent B) using a total flow rate of 0.25 mL/min. The chromatographic separation was achieved using a 5.0 min gradient elution. The initial mobile phase composition was 35% B, increasing to 90% B over 4 min, and finally brought back to the initial conditions of 35% B in 0.10 min, followed by 1 min re-equilibration. The injection volume (5 μL) was consistent for all samples.

Mouse Plasma Stability. The tested compounds were dissolved in DMSO to yield 2.5 mM solutions. Mouse plasma was diluted to 80% with PBS and heated at 37 °C before the assay. The tested compounds were incubated with the preheated plasma solution (final concentration: 50 μM) in a shaking water bath at 37 °C at six different time points: 0, 15, 30, 60, 90, and 120 min. Experiments were independently conducted in triplicate. At the end of the incubation time, 50 μL of sample was collected and mixed with 200 μL of cold acetonitrile to stop the reaction. Solutions were vortex-mixed and then centrifuged at 4 °C and 14 000 rpm for 15 min. Supernatants were diluted in methanol−water (50:50 v/v) and analyzed by HPLC−PDA-ESI-SQ-MS. Peak areas of test compounds were computed for each incubation time and relative levels to time zero are reported. Enalapril was used as a positive control during incubation.

SGF Stability. The tested compounds were dissolved in DMSO to yield 1 mM. Compounds were incubated with SGF solution (final concentration, 50 mM) in a shaking water bath at 37 °C for four different time points: 0, 30, 60, and 120 min. Experiments were independently conducted in triplicate. At the end of the incubation, 125 μL of sample solution was taken and 375 μL of acetonitrile was added to stop the reaction. The solutions were vortex-mixed and centrifuged at 25 °C and 15 000 rpm for 15 min. The supernatant was diluted in methanol−water (50:50 v/v) and analyzed by HPLC−MS. The percentage of compound remaining at the individual time points relative to the 0 min sample is reported based on the peak area of the test compound.

The HPLC−PDA-ESI-SQ-MS analysis was performed using a Waters Alliance e2695 system with a Phenomenex Kinetex XB-C18 (4.6 mm × 150 mm, 5 μm particle size) column, coupled to a Waters 2998 photodetector array and a Waters SQD2 single quadrupole mass spectrometer with an ESI source. Gradient elution was utilized in the chromatographic separation method using 0.1% formic acid in water (mobile phase A) and methanol (mobile phase B), with the following program: 0−9 min 75% B; 9−10 min 75−95% B; 10 min 95% B. The flow rate was constant at 0.4 mL min^{-1}. After each sample injection, the gradient was returned to its initial condition in 16 min. The injection volume was 5 μL, and the column temperature was 40 °C. The mass spectrometer was operated in positive ion mode with a probe capillary voltage of 3.0 kV. The sampling cone voltage was set to 45.0 V. The source and desolvation gas temperatures were set at 150 and 350 °C, respectively. The nitrogen gas desolvation flow rate was 600 L h^{-1}, and the cone gas flow rate was 10 L h^{-1}. The mass spectrometer was calibrated across the range of *m/z* 20−2023 with a sodium and cesium iodide solution. Data were acquired in scan mode with a scan duration of 0.2 s; in SIR mode for each test compound based on the *m/z* value for $[M + H]^+$ adduct ions and with unit resolution. Data acquisition and processing were conducted using MassLynx, version 4.1 (Waters Corp.).

■ ASSOCIATED CONTENT

Supporting Information

The Supporting Information is available free of charge at https://pubs.acs.org/doi/10.1021/acs.jmedchem.0c00371.

Additional synthetic pathways; chlamydial immunofluorescence images; HPLC traces, MS and NMR spectra; and purified protein examples (PDF)

Additional ClpP activity data (oligomerization, casein degradation, peptide degradation) (CSV)

■ AUTHOR INFORMATION

Corresponding Authors

Scot P. Ouellette − *Department of Pathology and Microbiology, College of Medicine, University of Nebraska Medical Center, Omaha, Nebraska 68198, United States*; Phone: 402-559-0763; Email: scot.ouellette@unmc.edu

Martin Conda-Sheridan − *Department of Pharmaceutical Sciences, College of Pharmacy, University of Nebraska Medical Center, Omaha, Nebraska 68198, United States*; orcid.org/0000-0002-3568-2545; Phone: 402-559-9361; Email: martin.condasherida@unmc.edu

Authors

Mohamed A. Seleem − *Department of Pharmaceutical Sciences, College of Pharmacy, University of Nebraska Medical Center, Omaha, Nebraska 68198, United States*; orcid.org/0000-0003-4379-5133

Nathalia Rodrigues de Almeida − *Department of Chemistry, College of Arts and Sciences, University of Nebraska at Omaha, Omaha, Nebraska 68182, United States*; orcid.org/0000-0002-9552-1233

Yashpal Singh Chhonker − *Clinical Pharmacology Laboratory, Department of Pharmacy Practice and Science, College of Pharmacy, University of Nebraska Medical Center, Omaha, Nebraska 68198, United States*; orcid.org/0000-0001-6455-5388

Daryl J. Murry − *Clinical Pharmacology Laboratory, Department of Pharmacy Practice and Science, College of Pharmacy, University of Nebraska Medical Center, Omaha, Nebraska 68198, United States*; orcid.org/0000-0002-4169-5027

Zaira da Rosa Guterres − *Laboratory of Cytogenetics and Mutagenesis, State University of Mato Grosso do Sul, Mundo Novo, Matto Grasso do Sul, Brazil*

https://dx.doi.org/10.1021/acs.jmedchem.0c00371
J. Med. Chem. 2020, 63, 4370−4387

Amanda M. Blocker − *School of Biological Sciences, Southern Illinois University Carbondale, Carbondale, Illinois 62901, United States*
Shiomi Kuwabara − *School of Biological Sciences, Southern Illinois University Carbondale, Carbondale, Illinois 62901, United States*
Derek J. Fisher − *School of Biological Sciences, Southern Illinois University Carbondale, Carbondale, Illinois 62901, United States;* orcid.org/0000-0002-1663-8389
Emilse S. Leal − *Centro de Investigaciones en BioNanociencias (CIBION), Consejo Nacional de Investigaciones Científicas y Técnicas (CONICET), 2390 Ciudad de Buenos Aires, Argentina*
Manuela R. Martinefski − *Centro de Investigaciones en BioNanociencias (CIBION), Consejo Nacional de Investigaciones Científicas y Técnicas (CONICET), 2390 Ciudad de Buenos Aires, Argentina;* orcid.org/0000-0002-4501-3783
Mariela Bollini − *Centro de Investigaciones en BioNanociencias (CIBION), Consejo Nacional de Investigaciones Científicas y Técnicas (CONICET), 2390 Ciudad de Buenos Aires, Argentina;* orcid.org/0000-0002-8718-6236
María Eugenia Monge − *Centro de Investigaciones en BioNanociencias (CIBION), Consejo Nacional de Investigaciones Científicas y Técnicas (CONICET), 2390 Ciudad de Buenos Aires, Argentina;* orcid.org/0000-0001-6517-5301

Complete contact information is available at: https://pubs.acs.org/10.1021/acs.jmedchem.0c00371

Notes

The authors declare no competing financial interest.

■ ACKNOWLEDGMENTS

This work was supported by the National Institute of Health-NIGMS, Nebraska Center for Molecular Target Discovery and Development (Grant 1P20GM121316-01A1; PI, Robert Lewis; Project Leader, Martin Conda-Sheridan), the Department of Defense-Peer Reviewed Medical Research Program 2017 (Grant W81XWH-18-1-0113, Martin Conda-Sheridan), and the National Science Foundation (CAREER Award 1810599 to Scot P. Ouellette). María Eugenia Monge and Mariela Bollini are research staff members from CONICET (Consejo Nacional de Investigaciones Científicas y Técnicas), Argentina.

■ ABBREVIATIONS USED

EB, elementary body; RB, reticulate body; STI, sexually transmitted infection; STDs, sexually transmitted diseases; ACP, activators of cylindrical protease; PyBOP, benzotriazole-1-yl-oxy-tris-pyrrolidino-phosphonium hexafluorophosphate; HBTU, *N,N,N′,N′*-tetramethyl-O-(1H-benzotriazol-1-yl)-uronium hexafluorophosphate; HATU, 1-[bis-(dimethylamino)methylene]-1H-1,2,3-triazolo[4,5-b]-pyridinium 3-oxid hexafluorophosphate; DIPEA, *N,N* diisopropylethylamine; IFA, immunofluorescence assay; IFU, inclusion forming unit; Hep-2, human epithelial type 2; HBD, hydrogen bond donor; HBA, hydrogen bond acceptor; SDS, sodium dodecyl sulfate; Suc-Luc-Tyr-AMC, succinic acid-leucin-tyrosin-7-amino-4-methyl-2H-chromen-2-one; TLC, thin layer chromatography; brs, broad signal; DMEM, Dulbecco's modified eagle medium

■ REFERENCES

(1) Centers for Disease Control. *New CDC Analysis Shows Steep and SPrevention. New CDC Analysis Shows Steep and Sustained Increases in STDs in Recent Years*. 2017, https://www.cdc.gov/media/releases/2018/p0828-increases-in-stds.html (accessed 2018-08-28).
(2) Braxton, J.; Davis, D. W.; Emerson, B.; Flagg, E. W.; Grey, J.; Grier, L.; Harvey, A.; Kidd, S.; Kim, J.; Kreisel, K. *Sexually Transmitted Disease Surveillance 2017*. 2018, https://www.cdc.gov/nchhstp/newsroom/2018/2017-STD-surveillance-report.html (accessed 2018-09-25).
(3) Manavi, K. A Review on Infection with *Chlamydia Trachomatis*. *Best Pract. Res. Cl. OB* **2006**, *20*, 941−951.
(4) Hafner, L. M.; Pelzer, E. S. Tubal Damage, Infertility and Tubal Ectopic Pregnancy: *Chlamydia Trachomatis* and Other Microbial Aetiologies. In *Ectopic Pregnancy-Modern Diagnosis and Management*; IntechOpen, 2011; pp 13−44, DOI: 10.5772/21555.
(5) Darville, T.; Hiltke, T. J. Pathogenesis of Genital Tract Disease due to *Chlamydia Trachomatis*. *J. Infect. Dis.* **2010**, *201*, S114−S125.
(6) Workowski, K. A.; Berman, S. M. Centers for Disease Control and Prevention Sexually Transmitted Disease Treatment Guidelines. *Clin. Infect. Dis.* **2011**, *53*, S59−S63.
(7) Dalaker, K.; Gjønnaess, H.; Kvile, G.; Urnes, A.; Anestad, G.; Bergan, T. *Chlamydia Trachomatis* as a Cause of Acute Perihepatitis Associated with Pelvic Inflammatory Disease. *Sex. Transm. Infect.* **1981**, *57*, 41−43.
(8) Hatch, T. P.; Allan, I. t.; Pearce, J. Structural and Polypeptide Differences Between Envelopes of Infective and Reproductive Life Cycle Forms of Chlamydia spp. *J. Bacteriol.* **1984**, *157*, 13−20.
(9) Abdelrahman, Y. M.; Belland, R. J. The Chlamydial Developmental Cycle. *FEMS Microbiol. Rev.* **2005**, *29*, 949−959.
(10) Abdelrahman, Y.; Ouellette, S. P.; Belland, R. J.; Cox, J. V. Polarized Cell Division of *Chlamydia Trachomatis*. *PLoS Pathog.* **2016**, *12*, No. e1005822.
(11) Moore, E. R.; Ouellette, S. P. Reconceptualizing the Chlamydial Inclusion as a Pathogen-Specified Parasitic Organelle: an Expanded Role for Inc Proteins. *Front. Cell. Infect. Microbiol.* **2014**, *4*, 157.
(12) Schautteet, K.; De Clercq, E.; Vanrompay, D. *Chlamydia Trachomatis* Vaccine Research Through the Years. *Infect. Dis. Obstet. Gynecol.* **2011**, *2011*, 963513.
(13) de la Maza, L. M.; Zhong, G.; Brunham, R. C. Update on *Chlamydia Trachomatis* Vaccinology. *Clin. Vaccine Immunol.* **2017**, *24*, e00543-16.
(14) Langdon, A.; Crook, N.; Dantas, G. The Effects of Antibiotics on the Microbiome Throughout Development and Alternative Approaches for Therapeutic Modulation. *Genome Med.* **2016**, *8*, 39.
(15) Kjaer, H.; Dimcevski, G.; Hoff, G.; Olesen, F.; Østergaard, L. Recurrence of Urogenital *Chlamydia Trachomatis* Infection Evaluated by Mailed Samples Obtained at Home: 24 weeks' Prospective Follow up Study. *Sex. Transm. Infect.* **2000**, *76*, 169−172.
(16) Horner, P. J. Azithromycin Antimicrobial Resistance and Genital *Chlamydia Trachomatis* Infection: Duration of Therapy May be the Key to Improving Efficacy. *Sex. Transm. Infect.* **2012**, *88*, 154−156.
(17) Horner, P.; Saunders, J. Should Azithromycin 1 g be Abandoned as a Treatment For Bacterial STIs? The Case for and Against. *Sex. Transm. Infect.* **2017**, *93*, 85−87.
(18) Kong, F. Y.; Hocking, J. S. Treatment Challenges for Urogenital and Anorectal *Chlamydia Trachomatis*. *BMC Infect. Dis.* **2015**, *15*, 293.
(19) Good, J. A.; Kulén, M.; Silver, J.; Krishnan, K. S.; Bahnan, W.; Nunez-Otero, C.; Nilsson, I.; Wede, E.; de Groot, E.; Gylfe, Å; Bergström, S.; Almqvist, F. Thiazolino 2-Pyridone Amide Isosteres as Inhibitors of *Chlamydia Trachomatis* Infectivity. *J. Med. Chem.* **2017**, *60*, 9393−9399.
(20) Good, J. A.; Silver, J.; Nunez-Otero, C.; Bahnan, W.; Krishnan, K. S.; Salin, O.; Engström, P.; Svensson, R.; Artursson, P.; Gylfe, Å; Bergström, S.; Almqvist, F. Thiazolino 2-Pyridone Amide Inhibitors of *Chlamydia Trachomatis* Infectivity. *J. Med. Chem.* **2016**, *59*, 2094−2108.

(21) Mojica, S. A.; Salin, O.; Bastidas, R. J.; Sunduru, N.; Hedenstrom, M.; Andersson, C. D.; Nunez-Otero, C.; Engstrom, P.; Valdivia, R. H.; Elofsson, M.; Gylfe, A. *N*-Acylated Derivatives of Sulfamethoxazole Block Chlamydia Fatty Acid Synthesis and Interact with FabF. *Antimicrob. Agents Chemother.* **2017**, *61*, No. e00716-17.
(22) Sunduru, N.; Salin, O.; Gylfe, Å.; Elofsson, M. Design, Synthesis and Evaluation of Novel Polypharmacological Antichlamydial Agents. *Eur. J. Med. Chem.* **2015**, *101*, 595−603.
(23) Moreno-Cinos, C.; Goossens, K.; Salado, I. G.; Van Der Veken, P.; De Winter, H.; Augustyns, K. ClpP Protease, a Promising Antimicrobial Target. *Int. J. Mol. Sci.* **2019**, *20*, 2232.
(24) Culp, E.; Wright, G. D. Bacterial Proteases, Untapped Antimicrobial Drug Targets. *J. Antibiot.* **2017**, *70*, 366.
(25) Brotz-Oesterhelt, H.; Beyer, D.; Kroll, H.-P.; Endermann, R.; Ladel, C.; Schroeder, W.; Hinzen, B.; Raddatz, S.; Paulsen, H.; Henninger, K.; Bandow, J. E; Sahl, H.-G.; Labischinski, H. Dysregulation of Bacterial Proteolytic Machinery by a New Class of Antibiotics. *Nat. Med.* **2005**, *11*, 1082−1087.
(26) Frees, D.; Brøndsted, L.; Ingmer, H. Bacterial Proteases and Virulence. In *Regulated Proteolysis in Microorganisms*; Subcellular Biochemistry, Vol. *66*; Springer: Dordrecht, The Netherlands, 2013; pp 161−192, DOI: 10.1007/978-94-007-5940-4.
(27) McGillivray, S. M.; Tran, D. N.; Ramadoss, N. S.; Alumasa, J. N.; Okumura, C. Y.; Sakoulas, G.; Vaughn, M. M.; Zhang, D. X.; Keiler, K. C.; Nizet, V. Pharmacological Inhibition of the ClpXP Protease Increases Bacterial Susceptibility to Host Cathelicidin Antimicrobial Peptides and Cell Envelope-Active Antibiotics. *Antimicrob. Agents Chemother.* **2012**, *56*, 1854−1861.
(28) Gur, E.; Biran, D.; Ron, E. Z. Regulated Proteolysis in Gram-Negative Bacteria—How and When? *Nat. Rev. Microbiol.* **2011**, *9*, 839−848.
(29) Sauer, R. T.; Baker, T. A. AAA+ Proteases: ATP-Fueled Machines of Protein Destruction. *Annu. Rev. Biochem.* **2011**, *80*, 587−612.
(30) Konovalova, A.; Søgaard-Andersen, L.; Kroos, L. Regulated Proteolysis in Bacterial Development. *FEMS Microbiol. Rev.* **2014**, *38*, 493−522.
(31) Lavey, N. P.; Coker, J. A.; Ruben, E. A.; Duerfeldt, A. S. Sclerotiamide:The First Non-Peptide-Based Natural Product Activator of Bacterial Caseinolytic Protease P. *J. Nat. Prod.* **2016**, *79*, 1193−1197.
(32) Kirstein, J.; Hoffmann, A.; Lilie, H.; Schmidt, R.; Rübsamen-Waigmann, H.; Brötz-Oesterhelt, H.; Mogk, A.; Turgay, K. The Antibiotic ADEP Reprogrammes ClpP, Switching it From a Regulated to an Uncontrolled Protease. *EMBO Mol. Med.* **2009**, *1*, 37−49.
(33) Socha, A. M.; Tan, N. Y.; LaPlante, K. L.; Sello, J. K. Diversity-Oriented Synthesis of Cyclic Acyldepsipeptides Leads to the Discovery of a Potent Antibacterial Agent. *Bioorg. Med. Chem.* **2010**, *18*, 7193−7202.
(34) Carney, D. W.; Schmitz, K. R.; Truong, J. V.; Sauer, R. T.; Sello, J. K. Restriction of the Conformational Dynamics of the Cyclic Acyldepsipeptide Antibiotics Improves Their Antibacterial Activity. *J. Am. Chem. Soc.* **2014**, *136*, 1922−1929.
(35) Leung, E.; Datti, A.; Cossette, M.; Goodreid, J.; McCaw, S. E.; Mah, M.; Nakhamchik, A.; Ogata, K.; El Bakkouri, M.; Cheng, Y.-Q.; Wodak, S. J.; Eger, B. T.; Pai, E. F.; Liu, J.; Gray-Owen, S.; Batey, R. A.; Houry, W. A. Activators of Cylindrical Proteases as Antimicrobials: Identification and Development of Small Molecule Activators of ClpP Protease. *Chem. Biol.* **2011**, *18*, 1167−1178.
(36) Hinzen, B.; Raddatz, S.; Paulsen, H.; Lampe, T.; Schumacher, A.; Habich, D.; Hellwig, V.; Benet-Buchholz, J.; Endermann, R.; Labischinski, H.; Brotz-Oesterhelt, H. Medicinal Chemistry Optimization of Acyldepsipeptides of the Enopeptin Class Antibiotics. *ChemMedChem* **2006**, *1*, 689−693.
(37) Famulla, K.; Sass, P.; Malik, I.; Akopian, T.; Kandror, O.; Alber, M.; Hinzen, B.; Ruebsamen-Schaeff, H.; Kalscheuer, R.; Goldberg, A. L.; Brötz-Oesterhelt, H. Acyldepsipeptide Antibiotics Kill Mycobacteria by Preventing the Physiological Functions of the ClpP1P2 Protease. *Mol. Microbiol.* **2016**, *101*, 194−209.
(38) Arvanitis, M.; Li, G.; Li, D.-D.; Cotnoir, D.; Ganley-Leal, L.; Carney, D. W.; Sello, J. K.; Mylonakis, E. A Conformationally Constrained Cyclic Acyldepsipeptide is Highly Effective in Mice Infected with Methicillin-Susceptible and -Resistant Staphylococcus aureus. *PLoS One* **2016**, *11*, No. e0153912.
(39) Yu, A. Y. H.; Houry, W. A. ClpP: A Distinctive Family of Cylindrical Energy-Dependent Serine Proteases. *FEBS Lett.* **2007**, *581*, 3749−3757.
(40) Rodgers, A. K.; Wang, J.; Zhang, Y.; Holden, A.; Berryhill, B.; Budrys, N. M.; Schenken, R. S.; Zhong, G. Association of Tubal Factor Infertility with Elevated Antibodies to *Chlamydia Trachomatis* Caseinolytic Protease P. *Am. J. Obstet. Gynecol.* **2010**, *203*, 494.e7.
(41) Wood, N. A.; Chung, K. Y.; Blocker, A. M.; Rodrigues de Almeida, N.; Conda-Sheridan, M.; Fisher, D. J.; Ouellette, S. P. Initial Characterization of the Two ClpP Paralogs of *Chlamydia Trachomatis* Suggests Unique Functionality for Each. *J. Bacteriol.* **2019**, *201*, No. e00635-18.
(42) Pan, S.; Malik, I. T.; Thomy, D.; Henrichfreise, B.; Sass, P. The Functional ClpXP Protease of *Chlamydia Trachomatis* Requires Distinct ClpP Genes From Separate Genetic Loci. *Sci. Rep.* **2019**, *9*, 1−14.
(43) Neuwald, A. F.; Aravind, L.; Spouge, J. L.; Koonin, E. V. AAA+: A Class of Chaperone-like ATPases Associated with the Assembly, Operation, and Disassembly of Protein Complexes. *Genome Res.* **1999**, *9*, 27−43.
(44) Krüger, E.; Zühlke, D.; Witt, E.; Ludwig, H.; Hecker, M. Clp-Mediated Proteolysis in Gram-positive Bacteria is Autoregulated by the Stability of a Repressor. *EMBO J.* **2001**, *20*, 852−863.
(45) Baker, T. A.; Sauer, R. T. ClpXP, an ATP-Powered Unfolding and Protein-Degradation Machine. *Biochim. Biophys. Acta, Mol. Cell Res.* **2012**, *1823*, 15−28.
(46) Kanishchev, O. S.; Dolbier, W. R., Jr Ni/Ir-Catalyzed Photoredox Decarboxylative Coupling of S-Substituted Thiolactic Acids with Heteroaryl Bromides: Short Synthesis of Sulfoxaflor and Its SF5 Analog. *Chem. - Eur. J.* **2017**, *23*, 7677−7681.
(47) Valeur, E.; Bradley, M. Amide Bond Formation: Beyond the Myth of Coupling Reagents. *Chem. Soc. Rev.* **2009**, *38*, 606−631.
(48) Coste, J.; Le-Nguyen, D.; Castro, B. PyBOP®: A new Peptide Coupling Reagent Devoid of Toxic by-Product. *Tetrahedron Lett.* **1990**, *31*, 205−208.
(49) Lipinski, C. A.; Lombardo, F.; Dominy, B. W.; Feeney, P. J. Experimental and Computational Approaches to Estimate Solubility and Permeability in Drug Discovery and Development Settings. *Adv. Drug Delivery Rev.* **1997**, *23*, 3−25.
(50) Snape, T. J. A Truce on the Smiles Rearrangement: Revisiting an Old Reaction—the Truce−Smiles Rearrangement. *Chem. Soc. Rev.* **2008**, *37*, 2452−2458.
(51) Ishibashi, H.; Uegaki, M.; Sakai, M.; Takeda, Y. Base-Promoted Aminoethylation of Thiols with 2-Oxazolidinones: A Simple Synthesis of 2-Aminoethyl Sulfides. *Tetrahedron* **2001**, *57*, 2115−2120.
(52) Ishibashi, H.; Uegaki, M.; Sakai, M. A Simple Synthesis of *β*-amino Sulfides. *Synlett* **1997**, *1997*, 915−916.
(53) Chang, C.-e. A.; Chen, W.; Gilson, M. K. Ligand Configurational Entropy and Protein Binding. *Proc. Natl. Acad. Sci. U. S. A.* **2007**, *104*, 1534−1539.
(54) Fang, Z.; Song, Y. n.; Zhan, P.; Zhang, Q.; Liu, X. Conformational Restriction: An Effective Tactic in'Follow-on'-Based Drug Discovery. *Future Med. Chem.* **2014**, *6*, 885−901.
(55) Fields, K. A.; Hackstadt, T. The Chlamydial Inclusion: Escape from the Endocytic Pathway. *Annu. Rev. Cell Dev. Biol.* **2002**, *18*, 221−245.
(56) Volceanov, L.; Herbst, K.; Biniossek, M.; Schilling, O.; Haller, D.; Nölke, T.; Subbarayal, P.; Rudel, T.; Zieger, B.; Häcker, G. Septins Arrange F-Actin-Containing Fibers on the *Chlamydia Trachomatis* Inclusion and Are Required for Normal Release of the Inclusion by Extrusion. *mBio* **2014**, *5*, 1802−1814.
(57) Hakala, E.; Hanski, L.; Uvell, H.; Yrjönen, T.; Vuorela, H.; Elofsson, M.; Vuorela, P. M. Dibenzocyclooctadiene Lignans from Schisandra spp. Selectively Inhibit the Growth of the Intracellular

Bacteria Chlamydia Pneumoniae and *Chlamydia Trachomatis*. *J. Antibiot.* **2015**, *68*, 609.
(58) Marwaha, S.; Uvell, H.; Salin, O.; Lindgren, A. E.; Silver, J.; Elofsson, M.; Gylfe, Å. *N*-Acylated Derivatives of Sulfamethoxazole and Sulfafurazole Inhibit Intracellular Growth of *Chlamydia Trachomatis*. *Antimicrob. Agents Chemother.* **2014**, *58*, 2968−2971.
(59) Batey, R.; Cossette, M.; Datti, A.; Eger, B. T.; Fai, E. F.; Goodreid, J.; Gray-Owen, S. D.; Houry, W. A.; Leung, E.; Liu, J.; Nhieu, A. J. *Activators of Cylindrical Proteases*. WO 2012079164A1, 2011.
(60) Shang, S.; Xia, L.; Zhong, M.; Zhang, J.; Zhao, J.; Gong, X.; Mabey, D.; Wang, Q. In Vitro Effects of Spectinomycin and Ceftriaxone Alone or in Combination with Other Antibiotics Against *Chlamydia Trachomatis*. *Antimicrob. Agents Chemother.* **2005**, *49*, 1584−1586.
(61) Wyrick, P. B. *Chlamydia Trachomatis* Persistence In Vitro: An Overview. *J. Infect. Dis.* **2010**, *201*, S88−S95.
(62) Ouellette, S. P.; Karimova, G.; Subtil, A.; Ladant, D. Chlamydia Co-Opts the Rod Shape-Determining Proteins MreB and Pbp2 for Cell Division. *Mol. Microbiol.* **2012**, *85*, 164−78.
(63) Ridgway, G.; Owen, J.; Oriel, J. The Antimicrobial Susceptibility of *Chlamydia Trachomatis* in Cell Culture. *Sex. Transm. Infect.* **1978**, *54*, 103−106.
(64) Keat, A. C.; Maini, R. N.; Nkwazi, G. C.; Pegrum, G. D.; Ridgway, G. L.; Scott, J. T. Role of *Chlamydia Trachomatis* and HLA-B27 in Sexually Acquired Reactive Arthritis. *Br. Med. J.* **1978**, *1*, 605−7.
(65) Suchland, R.; Geisler, W.; Stamm, W. E. Methodologies and Cell Lines Used for Antimicrobial Susceptibility Testing of Chlamydia spp. *Antimicrob. Agents Chemother.* **2003**, *47*, 636−642.
(66) Somani, J.; Bhullar, V. B.; Workowski, K. A.; Farshy, C. E.; Black, C. M. Multiple Drug-Resistant *Chlamydia Trachomatis* Associated with Clinical Treatment Failure. *J. Infect. Dis.* **2000**, *181*, 1421−1427.
(67) Foschi, C.; Salvo, M.; Cevenini, R.; Marangoni, A. *Chlamydia Trachomatis* Antimicrobial Susceptibility in Colorectal and Endocervical Cells. *J. Antimicrob. Chemother.* **2018**, *73*, 409−413.
(68) Smelov, V.; Perekalina, T.; Gorelov, A.; Smelova, N.; Artemenko, N.; Norman, L. In Vitro Activity of Fluoroquinolones, Azithromycin and Doxycycline against *Chlamydia Trachomatis* Cultured from Men with Chronic Lower Urinary Tract Symptoms. *Eur. Urol.* **2004**, *46*, 647−650.
(69) Lau, C.-Y.; Qureshi, A. K. Azithromycin Versus Doxycycline for Genital Chlamydial Infections: a Meta-Analysis of Randomized Clinical Trials. *Sex. Transm. Dis.* **2002**, *29*, 497−502.
(70) Kong, F. Y. S.; Hocking, J. S. Treatment Challenges for Urogenital and Anorectal *Chlamydia Trachomatis*. *BMC Infect. Dis.* **2015**, *15*, 293.
(71) Unemo, M.; Del Rio, C.; Shafer, W. M. Antimicrobial Resistance Expressed by Neisseria gonorrhoeae: A Major Global Public Health Problem in the 21st Century. *Microbiol. Spectrum* **2016**, *4*, 4.
(72) Holmes, N. E.; Charles, P. G. P. Safety and Efficacy Review of Doxycycline. *Clin. Med.: Ther.* **2009**, DOI: 10.4137/CMT.S2035.
(73) Peyriere, H.; Makinson, A.; Marchandin, H.; Reynes, J. Doxycycline in the Management of Sexually Transmitted Infections. *J. Antimicrob. Chemother.* **2017**, *73*, 553−563.
(74) Whittles, L. K.; White, P. J.; Paul, J.; Didelot, X. Epidemiological Trends of Antibiotic Resistant Gonorrhoea in the United Kingdom. *Antibiotics* **2018**, *7*, 60.
(75) Wang, S. A.; Papp, J. R.; Stamm, W. E.; Peeling, R. W.; Martin, D. H.; Holmes, K. K. Evaluation of Antimicrobial Resistance and Treatment Failures for *Chlamydia Trachomatis*: A Meeting Report. *J. Infect. Dis.* **2005**, *191*, 917−923.
(76) Páez-Canro, C.; Alzate, J. P.; González, L. M.; Rubio-Romero, J. A.; Lethaby, A.; Gaitán, H. G. Antibiotics for Treating Urogenital *Chlamydia Trachomatis* Infection in Men and Non-Pregnant Women. *Cochrane Database Syst. Rev.* **2019**, 1.
(77) Sandoz, K. M.; Rockey, D. D. Antibiotic Resistance in Chlamydiae. *Future Microbiol.* **2010**, *5*, 1427−1442.
(78) Wilson, G.; Miles, A.; Knox, R.; Parker, M.; Macrae, A.; Meynell, G.; Meynell, E. *Topley and Wilson's Principles of Bacteriology and Immunity*, 5th ed., Vol. *2*; Williams & Wilkins Company: Baltimore, MD,1964.
(79) Redgrove, K. A.; McLaughlin, E. A. The Role of the Immune Response in *Chlamydia Trachomatis* Infection of the Male Genital Tract: A Double-Edged Sword. *Front. Immunol.* **2014**, *5*, 534.
(80) Graf, U.; Würgler, F.; Katz, A.; Frei, H.; Juon, H.; Hall, C.; Kale, P. Somatic Mutation and Recombination Test in Drosophila Melanogaster. *Environ. Mutagen.* **1984**, *6*, 153−188.
(81) Thomé, S.; Bizarro, C. R.; Lehmann, M.; Abreu, B. R. R. d.; Andrade, H. H. R. d.; Cunha, K. S.; Dihl, R. R. Recombinagenic and Mutagenic Activities of Fluoroquinolones in Drosophila Melanogaster. *Mutat. Res., Genet. Toxicol. Environ. Mutagen.* **2012**, *742*, 43−47.
(82) Kalghatgi, S.; Spina, C. S.; Costello, J. C.; Liesa, M.; Morones-Ramirez, J. R.; Slomovic, S.; Molina, A.; Shirihai, O. S.; Collins, J. J. Bactericidal Antibiotics Induce Mitochondrial Dysfunction and Oxidative Damage in Mammalian Cells. *Sci. Transl. Med.* **2013**, *5*, 192ra85−192ra85.
(83) Ohnishi, S.; Murata, M.; Ida, N.; Oikawa, S.; Kawanishi, S. Oxidative DNA Damage Induced by Metabolites of Chloramphenicol, an Antibiotic Drug. *Free Radical Res.* **2015**, *49*, 1165−1172.
(84) Houston, J. B.; Galetin, A. Methods for Predicting in Vivo Pharmacokinetics Using Data From in Vitro Assays. *Curr. Drug Metab.* **2008**, *9*, 940−951.
(85) Pang, K. S.; Rowland, M. Hepatic Clearance of Drugs. I. Theoretical Considerations of a "Well-Stirred" Model and a "Parallel Tube" Model. Influence of Hepatic Blood Flow, Plasma and Blood Cell Binding, and the Hepatocellular Enzymatic Activity on Hepatic Drug Clearance. *J. Pharmacokinet. Biopharm.* **1977**, *5*, 625−653.
(86) Beatty, W. L.; Byrne, G. I.; Morrison, R. P. Morphologic and Antigenic Characterization of Interferon Gamma-Mediated Persistent *Chlamydia Trachomatis* Infection In Vitro. *Proc. Natl. Acad. Sci. U. S. A.* **1993**, *90*, 3998−4002.
(87) Marwaha, S.; Uvell, H.; Salin, O.; Lindgren, A. E.; Silver, J.; Elofsson, M.; Gylfe, Å. N-acylated Derivatives of Sulfamethoxazole and Sulfafurazole Inhibit Intracellular Growth of *Chlamydia Trachomatis*. *Antimicrob. Agents Chemother.* **2014**, *58*, 2968−2971.
(88) Rodrigues de Almeida, N.; Han, Y.; Perez, J.; Kirkpatrick, S.; Wang, Y.; Sheridan, M. C. Design, Synthesis, and Nanostructure-Dependent Antibacterial Activity of Cationic Peptide Amphiphiles. *ACS Appl. Mater. Interfaces* **2019**, *11*, 2790−2801.
(89) Graf, U.; van Schaik, N. Improved High Bioactivation Cross for the Wing Somatic Mutation and Recombination Test in Drosophila melanogaster. *Mutat. Res./Envir. Muta.* **1992**, *271*, 59−67.
(90) Frei, H.; Würgler, F. E. Statistical Methods to Decide Whether Mutagenicity Test Data from Drosophila Assays Indicate a Positive, Negative, or Inconclusive Result. *Mutat. Res./Envir. Muta.* **1988**, *203*, 297−308.
(91) de Rezende, A. A. A.; Graf, U.; Guterres, Z. d. R.; Kerr, W. E.; Spanó, M. A. Protective Effects of Proanthocyanidins of Grape (Vitis Vinifera L.) Seeds on DNA Damage Induced by Doxorubicin in Somatic Cells of Drosophila Melanogaster. *Food Chem. Toxicol.* **2009**, *47*, 1466−1472.
(92) Chhonker, Y. S.; Chandasana, H.; Mukkavilli, R.; Prasad, Y. D.; Laxman, T. S.; Vangala, S.; Bhatta, R. S. Assessment of In Vitro Metabolic Stability, Plasma protein Binding, and Pharmacokinetics of E- and Z-Guggulsterone in Rat. *Drug Test. Anal.* **2016**, *8*, 966−975.

https://dx.doi.org/10.1021/acs.jmedchem.0c00371
J. Med. Chem. 2020, 63, 4370−4387